Hydrothermal Oxidation of Hydrogen Sulfide

Master Thesis

Alexandr Gerganov - CE4-1-F25

Aalborg University
Departments of Chemistry and Bioscience

Chemistry and Bioscience
Aalborg University
http://www.aau.dk

AALBORG UNIVERSITY
STUDENT REPORT

Title:
Hydrothermal Oxidation of Hydrogen Sulfide

Theme:
Hydrogen Sulfide removal in the oil and gas industry

Project Period:
September 2024 - May 2025

Project Group:
CE4-1-F25

Participant(s):
Alexandr Gerganov

Supervisor(s):
Marco Maschietti

Copies: 1

Page Numbers: 78

Date of Completion:
June 1, 2025

Abstract:

In the oil and gas industry, the presence of H_2S causes many problems, especially on the offshore installations, as space is limited for a removal process there. Today, the most practiced technique is the usage of scavengers. They react with the sulfide and then they are release in the sea. This process is not entirely safe for the aqueous environment. Another approach would be the use of a solvent in capturing the hydrogen sulfide and then oxidizing it, thus preventing harmful chemicals from reaching the seawater. The most suitable conditions for oxidation and the resulting compounds are key factors in the process.

Preface

This project is written by Alexandr Gerganov, as part of the third and fourth semester of the Master in Chemical Engineering, completed at Aalborg University Esbjerg. The thesis was completed in the period September 2024 - May 2025 and presented in June 2025.

Aalborg University, June 1, 2025

Alexandr Gerganov

Contents

Chapter 1

Introduction

The oil and gas industry has had an extensive journey, starting in 1847 in current Baku, Azerbaijan. It is specifically there that the first commercial well was drilled [1]. Since then, fossil fuels and petrochemicals have become essential to society, providing a basis for economic growth and technological development.

Like any other industry, it has several problematic aspects. One of those is the formation of hydrogen sulfide (H_2S) in underground hydrocarbon reservoirs. There are many causes for it, such as natural occurrence or artificial induction by injection of water. In the end, the presence of hydrogen sulfide represents a problem because of its toxicity even in small amounts, as well as its corrosive activity on steel equipment in the presence of an aqueous environment. It acts as a weak acid, where it dissolved into bisulfides. Moreover, the laws of many countries specify limits for H_2S concentrations in natural gas for commercialization, due to its toxicity and the formation of SO_2 when burned. In the United States, the limit represents 4 ppmv (parts per million volume), which is equivalent to 0.25 grams per 100 scf (square cubic feet). In other countries, the limits are even lower, down to 1 ppmv [2]. Those requirements arise from several considerations:

- Toxicity - the OSHA (Occupational Health and Safety Administration) has a ceiling for H_2S exposure at 20 ppm. The gas has a specific smell of rotten eggs, detectable at concentrations as low as 0.5 ppb [3].
- Equipment corrosion - the presence of hydrogen sulfide in an aqueous medium causes an accelerated oxidation of steel pipelines [4].
- Environmental concerns - the presence of H_2S in natural gas results in its release into the atmosphere in form of SO_2 when the gas is burned. This will cause acid rains, which affect the vegetation and water bodies.

As a result, the formation and presence of H_2S in petrochemical reservoirs has been extensively studied. Depending on the reservoir, the sulfur content can

reach up to 5 wt% [5]. Factors like the composition of the reservoir rocks or the temperature also influence the sulfur formation (see more in section 2.1). The biggest output of the petroleum industry remains, however, water. Researchers at Argonne estimated that in 2007 the daily production of the industry in the United States constitutes 5 million barrels of oil, 67 billion cubic feet of natural gas, and 55 million barrels of water. Hence, the presence of water in the process is imminent, which facilitates the corrosive effects of H_2S [5].

Therefore, the development of techniques for the removal of H_2S from gas streams is a major research topic. Different reservoirs have different hydrogen sulfide concentrations and, consequently, different demands for the removal. The topic of removal of H_2S in offshore oil and gas installations is of particular interest. Due to difficulties arising from the limited space on the offshore platforms, as well as difficulties in operation, the applied mechanisms there vary from those employed on the onshore facilities. The most widely used method is H_2S scavenging, which implies injection of the so-called "H_2S scavengers", which react with H_2S, forming new compounds. Therefore, the most practical option in the offshore circumstances is to release the scavengers into the sea, which are usually liquid solutions. The latter are considered less dangerous than the H_2S. There are governmental regulations regarding what scavengers can be release and in what amounts. Usually, different companies have their own scavengers, which have to comply with the regulations.

A typical topside offshore process in the North Sea can be seen below in figure 1.1:

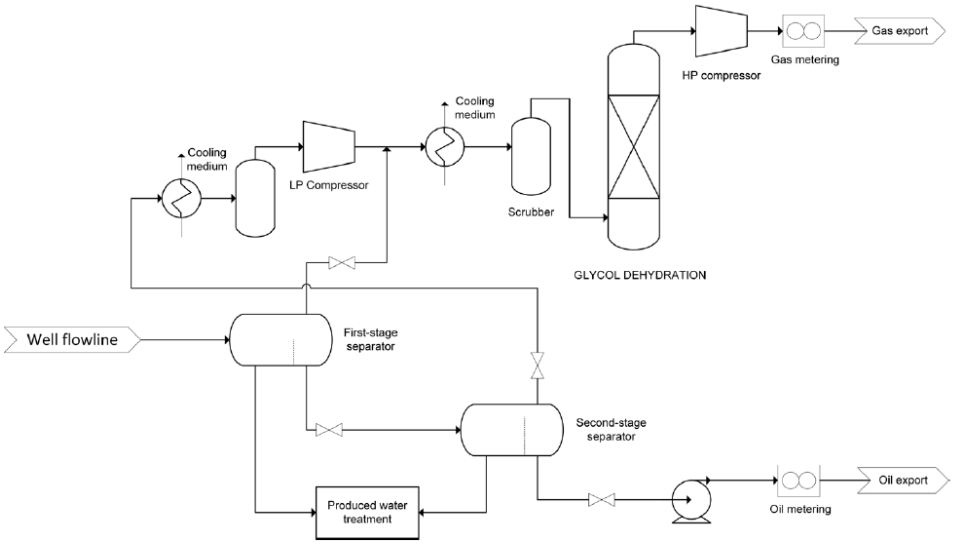

Figure 1.1: Conventional offshore topside process [5]

The well fluid is a mixture of oil, gas and water. After an initial separation into

liquid and gas phases, the gas is sent to a compressor. There it is subjected to the removal H_2S and CO_2. The liquid is sent to further separation of oil from water. In the end, both oil and gas are sent to export.

Alternatives in which scavengers are not applied are of interest. There already are existing methods for capturing acid gases, such as solvent regenerative methods. There, H_2S is captures by a solvent (such as amine based) and then regenerated. The process however would be challenging to implement offshore, due to space requirements and process complexity.

Possible alternatives to that include using solvents in a non regenerative way. One of those would be the absorption of H_2S in a basic solution, which will form bisulfide ions HS^-, which can treated by wet oxidation. However, it is a challenging idea, with many solvents available, each having its own advantages and disadvantages. At the same time, the implementation of this method offshore requires specialized equipment and site modifications, which are always challenging in offshore circumstances.

Chapter 2

Problem Analysis. H_2S in oil and gas industry

Hydrogen Sulfide, which naturally occurs in environments such as minerals (topaz or granite), salt mines, volcanoes, water bodies, and hydrocarbon reservoirs. The last is of particular interest because of the large production scale of the petrochemical industry.

2.1 Formation of H_2S in oil and gas reservoirs

The formation of hydrogen sulfide in oil and gas reservoirs can be attributed to the following processes:

Thermochemical Sulfate Reduction: At increased temperatures (>120°C), which occur in the hydrocarbon reservoirs, the sulfate contained in the injected seawater to maintain the well pressure, pore water or calcium sulfate can undergo reduction by components such as alcohols, polar aromatic and saturated hydrocarbons. This can result in high H_2S concentrations [6].

Aquathermolysis occurs at a temperature below 120 °C and the reaction between steam and sulfur-containing compounds present in oil, such as thiols or thiophenes, occurs [6]. As a result, hydrogen sulfide is produced. The water in reservoirs is most often injected by operators to maintain the pressure in the reservoir and extract more oil.

Oxidative and Reductive Dissolution of Metal Sulfides - Sulfide minerals are naturally contained in some reservoirs. Iron sulfides, such as pyrite, are among the most abundant. At acidic conditions (pH<7), pyrite decomposes into H_2S. The pore water contained in the reservoirs has the potential to absorb and retain amounts of H_2S. As the reservoir pressure decreases, the solubility of sulfide in water drops, and as a consequence gets release in the produced fluids [6].

Bacterial Sulfate Reduction (BSR) is a process facilitated by anaerobic microorganisms that reduce sulfate. Those are either already present in the reservoir are are introduced by water flooding [6].

The different mechanisms of "reservoir souring" can act independently or in tandem, depending on the circumstances.

It is worth mentioning that there are also techniques for preventing or slowing down the formation of H_2S. The most obvious is the use of water with a low sulfur content to maintain pressure in the wells. However, this is challenging in offshore conditions, where the most abundant source is sulfur-containing seawater, with about 2800 ppm [7]. Sulfur ions can also be removed from seawater using membrane technology. Although it is a promising technology, this is not widely practiced today.

Injection of biocide is another method to prevent or slow the formation of H_2S. Biocides are chemicals that prevent or control the growth of sulfur-reducing bacteria [7]. Biocides are widely used for this purpose in the oil and gas industry. They also prevent other harmful microorganisms from growing.

Aging of hydrocarbon reservoirs

Another issue of the modern oil and gas industry is the aging of the hydrocarbon reservoirs. A lot of reservoirs have been exploited since the 1970's. With time, the pressure in the reservoir decreases and more and more water was injected to maintain the pressure. Due to that, the effects of the hydrogen sulfide formation methods are enhanced. The injected water "washes" the oil from the underground rocks. At the same time, the minerals present in the reservoir, like pyrite, also get dissolved and with the assistance of the sulfur reducing bacteria are converted into H_2S. Therefore, the amount of hydrogen sulfide usually increases with time. Nowadays, as many of the old reservoirs are becoming more mature, their souring is also becoming more prominent. This requires more efforts in the removal of the H_2S [8]. This causes more scavengers to be used, which only enhances their total environmental impact.

2.2 Properties of H_2S

Hydrogen Sulfide (H_2S), also called monosulfane, is an inorganic compound. It is present primarily as a gas in the atmosphere, which is colorless, heavier than air and has a characteristic rotten egg smell [9].

In the following table 2.1, some basic properties of H_2S are presented [9]:

Table 2.1: Properties of H_2S

Property	Value
CAS number	7783-06-4
Molecular Weight	34.08
Boiling point (101.3 kPa)	-60.28 °C
Density (0°C)	1.539 g/ml
Vapor Pressure (0 °C)	10.32 bar
Solubility in water (20°C, pH = 7)	3.98 g/l

The chemical bond of hydrogen sulfide is shown below in Figure 2.1. Due to its ability to donate a proton, H_2S is a Brønsted-Lowry acid. The 2 hydrogen atoms form covalent bonds with the sulfur.

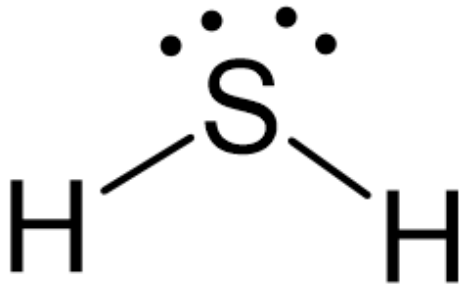

Figure 2.1: Electronic structure of H_2S

Due to the strong dipole, the hydrogen atoms are positioned at an angle of 92.1 degrees.

In aqueous solutions, H_2S is a weak acid with with the following dissociation [9]:

$$H_2S \rightleftharpoons HS^- + H^+, \qquad K_1 = 10^{-7}(18^\circ C) \tag{2.1}$$

The solubility of H_2S in water is dependent on the pH. At values greater than 7, the solubility is higher than in acidic environments [10].

Also, at different pH level different sulfide forms are noticed. As can be seen in Figure 2.2 below, at acidic pH the molecular H_2S form is present. In the range between neutral pH and 12, the bisulfide ion (HS^-) is present. At extreme basic pH, S^- is formed. Therefore, the present compound depends strictly on the acidity of the medium.

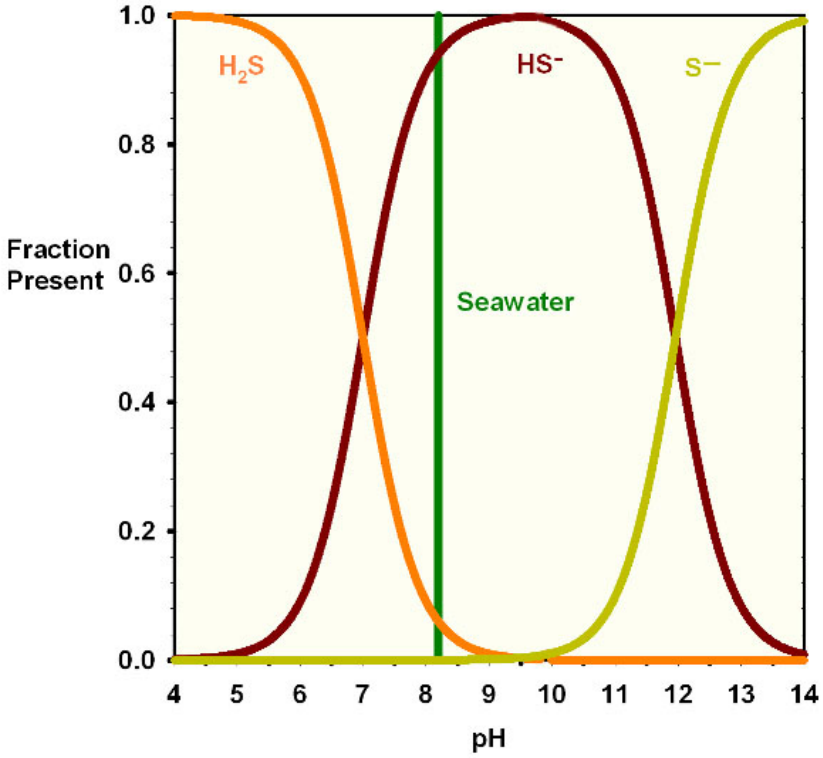

Figure 2.2: Speciation of hydrogen sulfide as a function of pH

H_2S and Corrosion

As mentioned before, one of the main problems linked to the H_2S presence in hydrocarbons is its corrosive activity. However, its corrosive activity is only significant in the presence of water [11]. In aqueous media, hydrogen sulfide dissociates into hydronium cations, as presented below:

$$H_2S + H_2O \leftrightarrows H_3O^+ + HS^- \tag{2.2}$$

Later, the bisulfide ion contributes to the formation of another hydronium cation:

$$HS^- + H_2O \leftrightarrows H_3O^+ + S^{2-} \tag{2.3}$$

The previous 2 reactions create a cathodic zone. A difference in charge is now created, with the iron from the pipe wall losing electrons [11]. Corrosion occurs when electrons flow from the anode to the cathode, which occurs here:

$$Fe \rightarrow F^{2+} + 2e^- \tag{2.4}$$

$$Fe^{2+} + 2H_3O^+ + S^{2-} \rightarrow FeS + H_2 \tag{2.5}$$

Iron sulfide deposits as corrosion products on the wall of the internal pipe [11]. A schematic image of the process can be seen in figure 2.3:

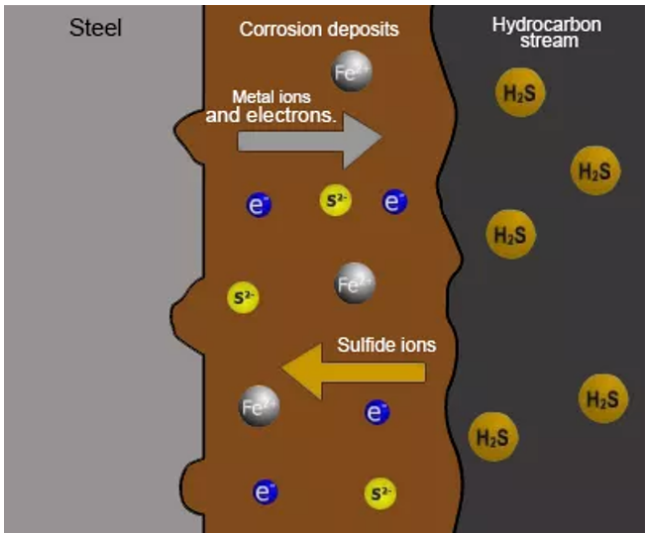

Figure 2.3: Mechanism of wet H_2S corrosion damage [11]

The corrosion levels are monitored by the oil and gas platform operators using different mechanisms to control the thickness of the pipe wall. Regular inspections and maintenance are also meant to ensure that corrosion levels do not affect the integrity of the platform.

2.3 Removal of H_2S from hydrocarbons with solvents

The removal of hydrogen sulfide, as mentioned before, is a problem present in the petrochemical industry. Throughout the evolution of the industry, various techniques have been developed to remove the H_2S from natural gas. The most well-known techniques are within chemical absorption.

2.3.1 Amine based solvents

Alkanolamines are the most widely used in gas sweetening processes (removal of acid gases). They are known for their effectiveness in removing various amounts of hydrogen sulfide or carbon dioxide and low operating cost.

The reactions between amines and acid gases such as H_2S have the following scheme:

1. Ionization and Hydrolysis:

$$H_2S \rightleftharpoons H^+ + HS^- \tag{2.6}$$

The presence of H_2S in an aqueous solution shifts the pH below 7. However, with a dissociation constant of $K_a = 3 \cdot 10^{-7}$ for H_2S the formation of bisulfide will occur:

$$H_2S + OH^- \rightleftharpoons HS^- + H_2O \tag{2.7}$$

2. Protonation of amines

Amines can be primary, secondary, or tertiary. A representation of those can be seen in figure 2.4:

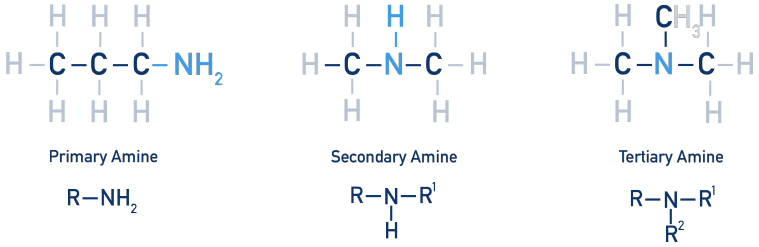

Figure 2.4: The 3 types of amines [12]

Below, the protonation reaction of a primary amine in an acidic environment can be seen:

$$RNH_2 + H^+ = RNH_3^+ \tag{2.8}$$

The formation of RNH_3^+ depends on the pH. Although amines have equilibrium constants in the range of 10^8, which facilitates the formation of the protonated ion. However, a higher pH interferes with its formation.

3. Reactions with H_2S

There are 2 mechanisms for the raection between the sulfide and the amine components:

$$RNH_3^+ + HS^- = RNH_3 \cdot SH \tag{2.9}$$

$$RNH_2 + H_2S = RNH_3 \cdot SH \tag{2.10}$$

The first reaction is faster, but the second one occurs at a higher pH, when the formation of the protonated ion is limited.

There are several amine solvents that have been used primarily in the capture of H_2S.

Monoethanolamine (MEA)

MEA was one of the first alkanolamines used in hydrogen sulfide absorption processes. It is mainly used as diluted aqueous solutions to absorb smaller amounts of H_2S. It is the most reactive, volatile, and corrosive alkanaloamine. Primary amines like MEA are known to form stronger acid-gas bonds, which makes their regeneration more challenging [2].

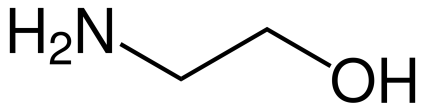

Figure 2.5: The structure of Monoethanolamine

MEA is also known to have low hydrocarbon absorbivity, which is quite important when capturing H_2S from natural gas streams. A solution of 15-20 wt% of MEA can capture up to 0.4 moles of H_2S per mole of amine [2].

Diethanolamine (DEA)

DEA is a secondary amine. It is widely used in gas sweetening processes. DEA is less corrosive than MEA, allowing for it to be used at higher concentrations and for the capture of higher H_2S gas concentrations. DEA is also known to be resistant to degradation from RSH or COS [2].

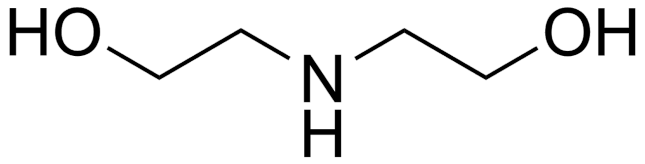

Figure 2.6: The structure of Diethanolamine

DEA has moderate hydrocarbon absorbivity, is not selective of H_2S, but has lower corrosivity than MEA. At a concentration of 20-35 wt%, up to 0.6 moles of H_2S per mole of DEA can be absorbed [2].

Methyldiethanolamine MDEA

MDEA is a tertiary amine. It has gained popularity in recent decades, primarily due to its selectivity for H_2S over CO_2, which is particularly useful in streams

containing both gases. It has low corrosivity and low heat requirements, which mean the bond with the acid gas is not so strong.

Diglycolamine (DGA)

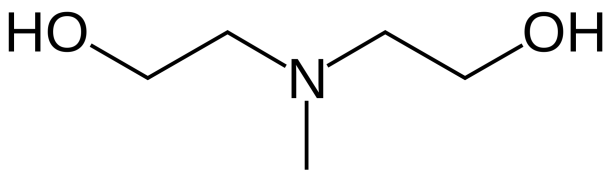

Figure 2.7: The structure of Methyldiethanolamine

MDEA can capture up to 0.45 moles of H_2S per moles of amine for a 40-55% solution. Unfortunately, it has high hydrocarbon absorbivity.

Industrial unit

In the Figure 2.8, a basic process of amine absorption process is presented.

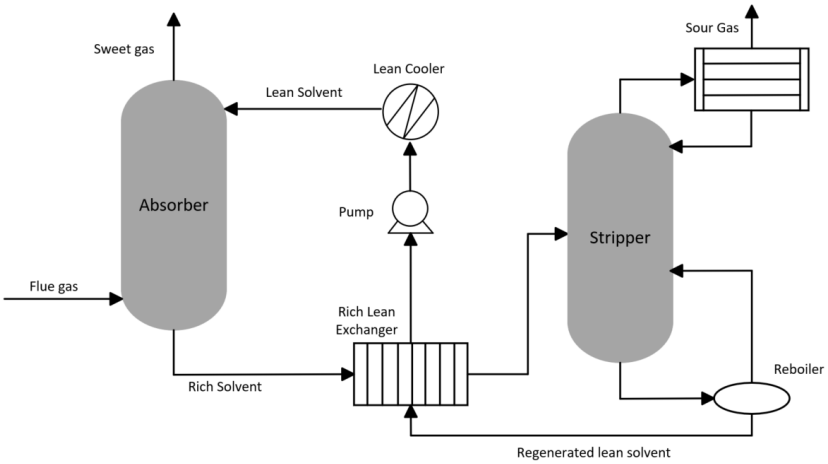

Figure 2.8: Basic amine absorption process unit [13]

In the process, the amine-based solvent, for example a 30 wt% MEA aqueous solution, is brought to contact with the sour gas in an absorber in counter current. This ensures a better contact surface between the solvent and the targeted gas. The temperature range in the absorption column for various amines is 35-50°C. Next, the rich solvent is regenerated in a stripping column, where the acid gases are recovered from the top. Typical temperatures in the stripper are in the 115-126 °C

range. Further, the clean solvent is recycled back to the process after being cooled [13].

2.3.2 Sodium Hydroxide Solution

Just like amine-based solvents, NaOH reacts with H_2S. In the exchange reaction between the two, sodium hydrosulfide or sodium solfide are formed:

$$NaOH + H_2S \rightleftharpoons NaSH + H_2O \tag{2.11}$$

$$2NaOH + H_2S \rightleftharpoons Na_2S + 2H_2O \tag{2.12}$$

The reaction occurs as long as the pH stays above 7. Once the pH becomes acidic, H_2S is released. Therefore, it is essential that NaOH is in excess at all times.

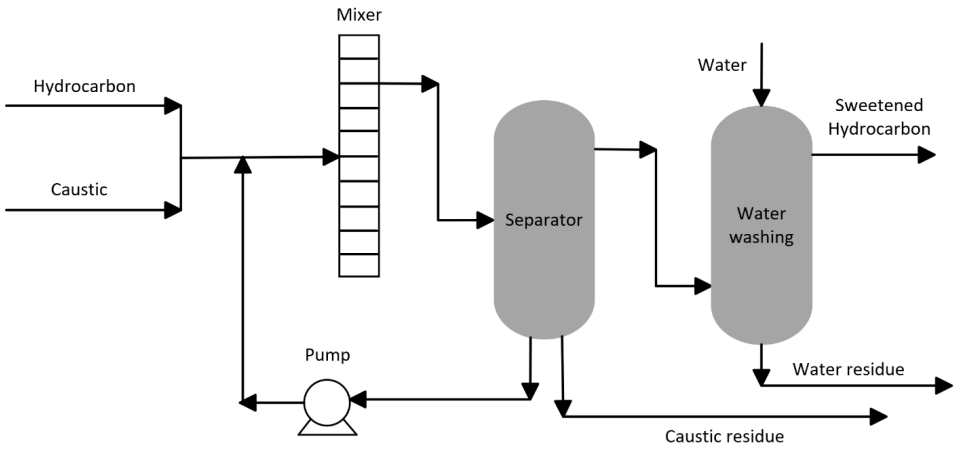

Figure 2.9: Schematical representation of a classical caustic treatment process [14]

In the depicted process, it can be seen that the hydrocarbon and caustic streams enter the mixer. Besides better mixing, it has the role of ensuring a bigger spread of droplets. Later, the mixture is sent to the separator, where the caustic solution is separated from the hydrocarbon mixture due to density differences. From the bottom of the column, part of the caustic solution is sent back to the mixer, where it is reintroduced to the system together with the fresh solution. The hydrocarbon mixture is sent to a water washing tower, where the remains of caustic soda are washed with water. In the end, the sweetened hydrocarbon is carried to the dehydration unit [14].

The usual concentrations of caustic soda in the aqueous caustic solutions usually is within the 5-15 wt% range.

A scientific study [15] researching methods to treat H_2S and CO_2 from sour gas by alkali describe a method of treating H_2S from gas streams using NaOH. They

prepared solutions of 0.01 up to 2 M. In the performed experiments, the sulfide gas was bubbled through the NaOHs solution for 60 minutes. The concentration of hydroxide was monitored as an indicator for the amount of absorbed sulfide. The concentration of HS^- ion varied at different concentrations of hydroxide. The highest value, however, was obtained with the 0.1 M solution of NaOH. During this experiment, the concentrations of HS^- in the solution was 0.4 mol/L [15].

In addition, the study also determined that at low concentrations of NaOH, both H_2S and HS^- were present in the solution. However, at higher hydroxide concentrations, the predominant species was the HS^- ion. This is due to the high basicity of the more concentrated NaOH solutions, which make the absorption of H_2S to take longer [15].

Both amine-based acid gas removal and caustic scrubbing are established industrial processes. The caustic scrubbing is less corrosive and cheaper. The amines, however, can be regenerated. Therefore, the coice depends on the process specifics.

2.3.3 Potassium Carbonate solution

Another solvent which can absorb H_2S is potassium carbonate (K_2CO_3). The reaction results in the formation of [16]

$$H_S + K_2CO_3 \rightleftarrows KHCO_3 + KHS \tag{2.13}$$

The process occurs at temperature in the range 70-130 $^\circ C$. When comparing the process to sodium hydroxide absorption, the potassium carbonate can be regenerated. When comparing the processes, however, sodium hydroxide has several advantages.

A comparison of different H_2S capture methods was done by Seo et al [17]. They determined that NaOH had an H_2S removal capacity 3 times higher than K_2CO_3. Sodium hydroxide is also more reactive than potassium carbonate at various conditions like flow rate or temperature. Hence, the main advantage of potassium carbonate remains its potential for regeneration.

2.4 Scavengers if offshore H_2S removal

Today, in offshore oil and gas installations, H_2S is treated by injecting liquid scavengers directly into the gas stream. Those are solutions of components that are highly reactive with H_2S. The reaction occurs as a gas-liquid reaction, where the sulfide reacts with the liquid droplets of the scavenger. The most widely used class of compounds for this purpose are the amines, particularly the triazines. The main advantages include low operating cost and solvent effectiveness.

Despite their large application, scavengers have not been extensively studied. The kinetics of those reactions are not entirely clear, which generates a lack of

mathematical models. As a result, it is challenging to predict the outcome of the reaction. All of the above-mentioned results in the ineffectiveness of the scavenging process [18]. As a result, large amount of scavenger are used, which results in excessive discharge.

Process description

The scavengers are usually injected in the high pressure gas streams, to ensure a better spread of the scavenger droplets and more contact surface. A representation of the injection process can be sene in figure 2.10:

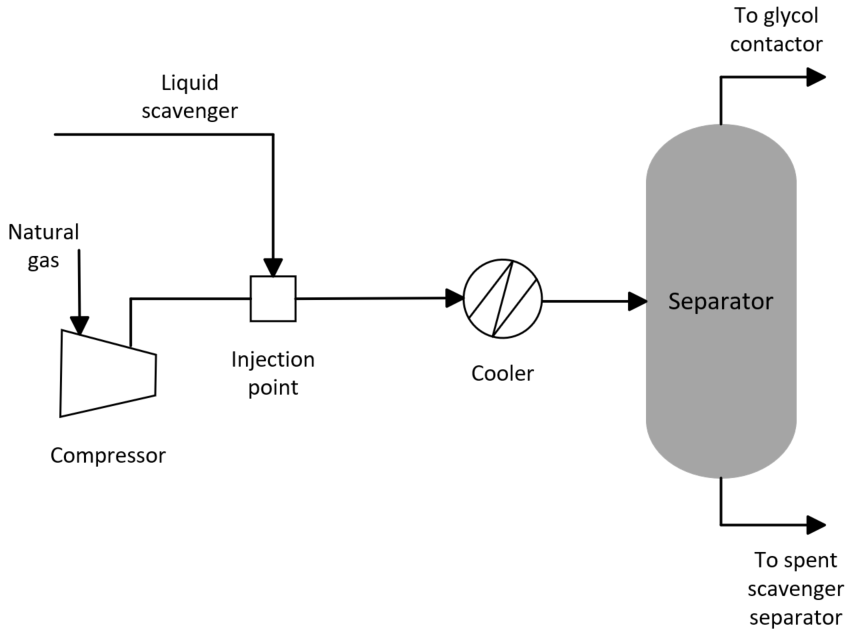

Figure 2.10: Topside process involving scavengers [19]

The temperature of the process can vary from ambient to $160°C$, depending on the scavenger. As it will be mentioned further in this section, at high temperatures some scavengers can manifest extended corrosion effects. The pH of the solution dispersed in the gas is usually 9-11. The process can be split into several steps:

- Diffusion of the H_2S through the liquid phase (scavenger solution)
- Absorption of H_2S into the aqueous scavenger solution
- Reaction between H_2S and the scavenger in the aqueous phase

The injection and dispersion a scavenger solution directly into the gas stream in a co-current manner. This helps minimize the space required by the setup, which is critical offshore. A schematic image of the process is presented in figure 2.11.

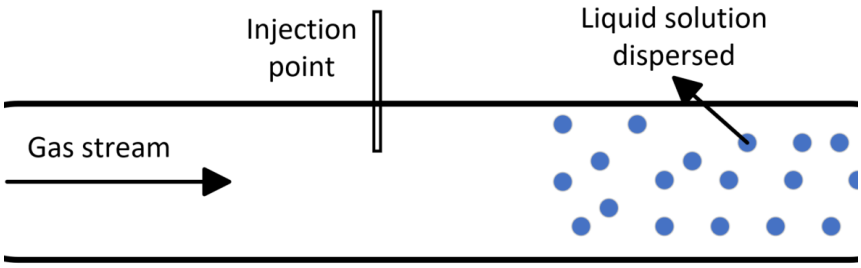

Figure 2.11: Co-current injection of scavenger in gas streams

The most widely used scavenger is MEA-triazine (scientific name: 1,3,5-tri- (2-hydroxyethyl) -hexahydro-S-triazine (HET)). It cover roughly 80% of the market. HET is largely preferred due to its high solubility in water, which applies also for its by-products and its scavenging efficiency.

Reaction scheme of MEA-triazine with H_2S

The reaction scheme can be viewed below:

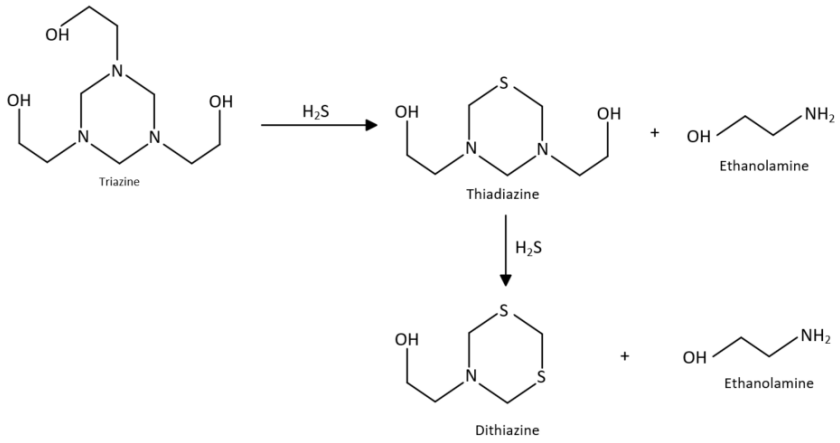

Figure 2.12: Reactions mechanism of HET with H_2S

Initially, H_2S dissolves in the liquid phase and HET is protonated. The reaction between those 2 results in the formation of thiadizine - an intermediate component and MEA. The reactions are:

$$HET + H_3O^+ \rightleftharpoons HET^+ + H_2O \tag{2.14}$$

$$H_2S(l) + H_2O \rightleftharpoons HS^- + H_3O^+ \tag{2.15}$$

$$HET^+ + HS^- \rightarrow TDZ + MEA \tag{2.16}$$

TDZ can further also undergo protonation and react with HS^-, forming DTZ and naother MEA molecule:

$$TDZ + H_3O^+ \rightleftharpoons TDZ^+ + H_2O \tag{2.17}$$

$$TDZ^+ + HS^- \rightarrow DTZ + MEA \tag{2.18}$$

The substitution of the last sulfur atom in the ring is normally not noticed. This is potentially due to the lack of nucleophilic carbon center for the HS^- attack in DTZ. Another component which can be involved further in the reaction chain is MEA:

$$MEA + H_3O^+ \rightleftharpoons MEA^+ + H_2O \tag{2.19}$$

In general, the absorption of H_2S causes the pH drop as protonated hydrogen atoms are generated. However, the scavenging reaction increases the pH as a result of the formation of monoethanolamine. The protonation of HET, TDZ and DTZ also tends to decrease the solution pH. At higher pH values there is a reduction in fractions of the protonated forms of HET, DTZ and TDZ, which inhibits the scavenging reaction. The reaction rate, therefore, depends strongly on the pH in addition to temperature.

The generated chemicals from the reaction are released in the sea. Their discharge in the aquatic environment is allowed in controllable amounts under surveillance. However, these components are not completely harmless to the environment. Therefore, a solution to combat the release of these chemicals into the sea is required.

The Gorm incident, 2001

As mentioned before, the scavengers can also be problematic for the integrity of the equipment on the offshore installations. One of the most prominent scavenger-related incidents happened in the danish sector of the North Sea, on the Gorm C platform. There, on 20th of May 2001, an explosion occurred due to a corroded gas pipeline on the platform. The incident resulted in an explosion, fortunately with

0 fatalities. The details of the incident and the investigation are described by Kim Rasmussen et. al in their paper [20].

Back in 2001, the produced gas from Gorm contained around 30-40 ppm of H_2S. After the reaction with the scavenger, the level dropped below 2 ppm. Since 1995 scavengers have been used on Gorm, primarily 1,3,5- tri(2-hydroxyethyl)-(2H,4H,6H)-hexahydro-1,3,5-Triazine (THET). The scavenger has been injected downstream of the IP compressor at process conditions of 135° C and 45 bar. The pH of the scavenger solution ranges usually within 10-11. Around 35 l/h are injected into a gas flow of 48 000 m^3/h. A corrosion monitoring program has been implemented, due to concerns regarding corrosion. However, as the water content in the gas was low (5%), the pipe was deemed safe from corrosion. The used chemicals offshore also have to undergo testing regarding corrosion. Only after passing the tests, they are allowed to be used.

Despite the precautions, the corrosion did gradually reduce the pipe thickness, until one day it leaked and found an ignition source. An extensive investigation has been performed, involving representatives from Maersk Oil A/S, Capcis Limited (consulting company specialized in corrosion) and The University of Aarhus. The more detailed corrosion tests performed by them resulted in the discovery that at temperatures from 130 to 150 °C, thermal degradation of the scavenger occurs. This lead to the formation of formic acid..

The above scavenger THET contained some N-(2-hydroxyethyl) formamide, which is a byproduct from its production. Its degradation pattern can be seen in the equation below:

$$CHO - NH - CH_2 - CH_2 - OH + H_2O \rightleftarrows HCOOH + NH_2 - CH_2 - CH_2 - OH \tag{2.20}$$

$$HCOOH + NH_2 - CH_2 - CH_2 - OH \rightleftarrows HCOO^{-+}BH_3 - CH_2 - CH_2 - OH \tag{2.21}$$

Further, in the presence of iron, H_2S and a base (MEA), irone formate could be formed, regenerating the formic acid:

$$Fe^{2+}(HCOO^-)_2 + H_2S \rightarrow FeS + 2HCOOH \tag{2.22}$$

The presence of iron sulfide and N-(2-hydroxyethyl) formamide on inside pipe wall suggests the presented reaction pattern to be true. This incident shows again how dangerous the corrosive properties of scavengers can be.

2.5 H_2S Scavengers. Environmental and practical concerns

The above mentioned incident from the Danish offshore sector is a reminder of the hazards scavengers carry. The lack of knowledge about their behavior at different

temperature is always to be taken into account.

The handling of scavengers in offshore circumstances is challenging. The wastewater stream which is generated after the H_2S absorption is of alkaline pH. There is also the risk of potential polymerization of Dithiazine (DTZ). This causes issues with fouling and scaling on equipment. Those issues are the primary driver behind the spent and unspent scavengers (SUS) being released in the sea, as other options are unavailable in offshore circumstances [19].

Despite the fact the controlled release of (SUS) in the sea is allowed, the triazine-based scavengers are not harmless to the aquatic life. According to the Danish Environmentla Portection Agency, various triazine compounds have LD50 values starting from 600 mg/kg for rats, which is comparable to methanol. The chemicals have also been linked to cancer tumors formation in animals [21].

The SUS also contain MEA from the reaction between the scavenger and H_2S. MEA is regarded as dangerous to aquatic life, with long lasting effects by the European Chemical Agency [22].

Stepanicev et al [23] claim that around 20% of the total environmental impact of the North Sea oil and gas platform is generated by the scavenger related activities. This data is from 2018. The initial impact of scavengers was smaller, but their usage with time increased proportionally to the H_2S concentration in reservoirs, which raised concerns about their environmental impact.

Another issue related to scavengers is the lack of knowledge regarding the absorption-reaction process with H_2S. hence, the oil and gas operators have to be conservative in their usage of scavengers, which results in large excess being used. Stoichiometrically, 6-8 kg of MEA-Triazine are needed to remove 1 kg of H_2S. In reality, 12-20 kg of commercial scavengers are used (40-50% aqueous solutions). As result, a large amount of scavenger never react and end up in the sea [24].

Chapter 3

Hydrothermal Oxidation

Water treatment is an important issue in the field of environmental science. Municipal sludge and the waste from various chemical processes generate the need for techniques that are able to degrade chemicals effectively. Hydrothermal oxidation (HTO), which uses water as a reactant and solvent, is a known technology that has some industrial applications, such as handling pharmaceutical waste or municipal usage, such as handling sewage water treatment. A type of HTO is the wet air oxidation (WAO).

3.1 Background of Wet Air Oxidation

It is applied in the temperature range between of 100 - 320 $^{\circ}C$, the boiling and critical point of water. The pressure range of the process is 5 - 200 bar. The increased pressure is required to keep water in liquid state. The usual oxidant choice is oxygen in form of air. Its increased solubility in aqueous solutions at elevated temperatures and pressures facilitates the oxidation process. The water facilitates the heat transfer and removes the excess heat via evaporation. The process allows neutralization of waste in the 20-200 g/l COD range. The oxidation products usually include low-mass molecules, such as CO_2, H_2O, SO_4 or NH_3, depending on the feed [25].

The primary factors to influence the extent of oxidation are:

- Temperature
- Oxygen concentration
- Residence time
- The chemical composition of the targeted pollutants

WAO is generally carried in a reactor, where the wastewater is heated and pressurized with oxygen (air). Wet air oxidation is suitable for waste concentrations that are too low for incineration but too high for biological treatment. The process can be applied to toxic waste that microorganisms cannot digest or is too hazardous to incinerate. A diagram of a classical hydrothermal oxidation plant can be viewed below in figure 3.1.

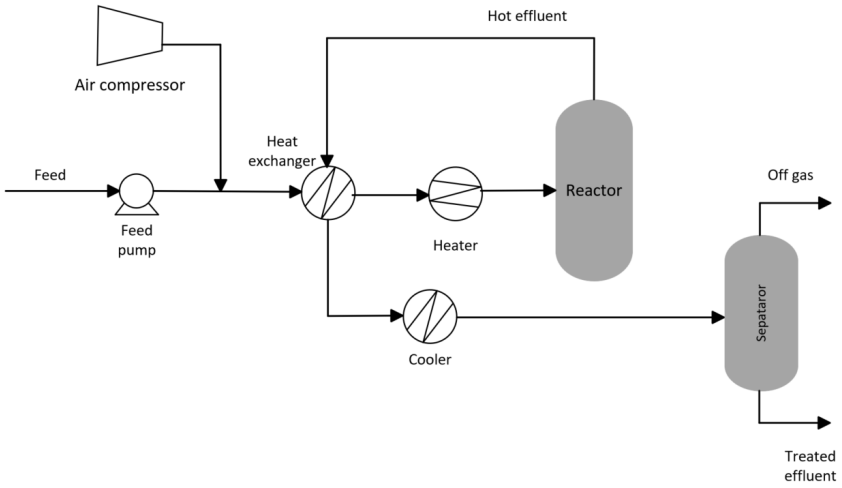

Figure 3.1: Typical flow diagram of HTO [25]

The feed is pumped into a heater, alongside air. The mixture goes into a reactor, where the oxidation occurs. The oxidized stream is cooled and sent to a separator, where the effluent is split from the gas. For energy efficiency, the system is equipped with heat exchangers.

The operating costs for wet oxidation are lower than those for incineration. On the other hand, the capital costs are higher. They depend on factors such as materials, flow rate, composition of wastewater, and extent of required oxidation [25].

The disadvantages include the possibility of corrosion, which induces a need for more resistant and expensive materials. Stainless steel, for example, is resistant to chloride concentrations of up to 300 mg/l. For higher amounts, titanium alloys prove to be better. Money can be saved on materials when flow rate is decreased, but this will consequently influence the productivity of the plant [25].

Most wet oxidation industrial facilities treat sewage sludge. This is performed under conditions below 473 K and results in COD reductions of 5-15%. However, it leads to improved sterility and filtering of the sludge. Wet air oxidation can also be used to regenerate activated carbon filters, with low impact on the carbon itself (only 1-5% losses) [25].

3.2 Kinetics and Mass Transfer

The necessary time for treatment and the reactor volume depend on the reactor type, rate of oxidation, and degree of oxidation. Faster oxidation is, of course, advantageous. The overal oxidation rate for a noncatalytic process is defined by 2 stages: the physical mass transfer of oxygen to the liquid phase and the chemical reaction between oxygen and the pollutants [25].

3.2.1 Stages of Wet Oxidation

Wet Oxidation consists of 2 main stages: a) the physical stage, where the oxygen is transferred from the gas to the liquid phase, and b) the chemical stage, where the transferred oxygen reacts with the targeted compounds.

Physical stage

In the physical stage, the most essential aspect is the transfer rate of oxygen into the liquid stage. The resistance occurs usually at the gas-liquid film interface. The 3 limiting scenarios include [25]:

- The oxygen reaction happens within the film
- O_2 reacts with the bulk solutions, where its concentration is negligibly close to 0
- The concentration of molecular oxygen is equal in both phases - the system has achieved equilibrium

If the mixing efficiency is very high, the rate of oxygen transfer to the liquid phase can be neglected. This enables the focus to be made on the more important chemical step rate.

Chemical Stage

The chemical stage consists of a series of reactions between dissolved oxygen, which oxidizes the compounds of interest. There is several factors that are to be considered, such as [25]:

- Temperature
- Partial Pressure of Oxygen (amount of dissolved O_2
- Reactor parameters (size, heating system etc.)
- pH of solution

- Nature of the targeted compounds

For a good diffusion of oxygen through the liquid, a reactor that ensures maximum mass transfer is desired.

Reaction Rate

Detailed studies on the kinetics of the oxidation and the reactor design is usually based on empirical calculations. Hence, the kinetics are described using the Arrhenius relation, pollutant concentration and concentration of oxygen [25]:

$$r_r = A \cdot e^{-(E/RT)} \cdot (C_P)^m \cdot (C_{O_2,L})^n \tag{3.1}$$

The reaction rate increases with temperature. r_r is the rate, A - the pre-exponential factor, E - activation energy, R - gas constant, T - temperature, C_p - pollutant concentration and $C_{O2,L}$ - oxygen concentration. m and n are reaction orders. An increase in temperature is met by a necessity for a pressure increase, as the equilibrium vapor pressure increases also with temperature. To maintain the system liquid, the pressure must be above the water vapor pressure for the corresponding temperature [25].

3.3 Wet Oxidation Pathways

Wet oxidation uses molecular oxygen in aqueous phase as means for radical production. The latter are essential in mineralization or decomposition of pollutants [26]. The reaction pathway can be described as follows:

$$RH + O_2 \rightarrow R^* + HO_2^- \tag{3.2}$$

$$RH + HO_2^- \rightarrow R^* + H_2O_2 \tag{3.3}$$

Further, the radicals can react with more oxygen atoms, until a large enough oxidation extent is achieved, that the reaction does not progress anymore:

$$R^* + O_2 \rightarrow ROO^* \tag{3.4}$$

These free radicals propagate the oxidation reactions through chain mechanisms, continually forming reactive intermediates (e.g., alcohols, aldehydes, carboxylic acids, sulfites) that further break down into smaller species, eventually leading to complete mineralization [26].

Wet air oxidation is a complex chemical process involving multiple steps, including free radical generation, oxidation of organic pollutants into smaller intermediates, and final conversion to harmless or less harmful substances. The process

is highly effective for degrading complex and refractory organic compounds in wastewater under controlled high-temperature and high-pressure conditions [26].

3.4 Oxidation of Hydrogen Sulfide (H_2S)

When H_2S is present in water, it can remain in its neutral form or become a bisulfide ion (HS^-, depending on the pH of the solution). The ionic form dominates at basic pH [15]. In any form, the sulfide can be oxidized while in an aqueous solution. This would allow to eliminate the hazardous H_2S that results from the petrochemical activity. In their paper called "The products from the oxidation of H_2S in seawater ", the authors describe the oxidation process of hydrogen sulfide in seawater, at lower temperatures (10-45$^\circ C$) [27].

Sulfur can have the oxidation numbers of -2, 0, +2, +4 and +6. Its higher oxidation state corresponds to sulfate, which is the theoretical final product of sulfur oxidation. However, the oxidation pathway does not proceed directly from sulfide to sulfate. Hence, there are several intermediate products. The oxidation of H_2S represents a series of reactions that result in the formation of reduced sulfur species, such as sulfate (SO_4^{2-}) - oxidation state of +6, sulfite (SO_3^{2-}) - oxidation state of +4, thiosulfate ($S_2O_3^{2-}$) - oxidation state of +2, and elemental sulfur (S) - oxidation state of 0 [27].

In their experiments, Zhang et. al analyzed the oxidation products at different pH values. The oxygen was in excess 10 times and reaction temperature was 25 $^\circ C$. The reaction time is reported as half time of the reaction, which is defined as the time needed for 50% of the bisulfide to be oxidized ($T_{1/2}$). The experiments were performed in a 1000 cm^3 water jacket glass, being heated by a Forma temperate bath. Essentially, the setup was similar to a batch reactor. The basicity level was maintained using a 0.002 bicarbonate solution. The sulfur-containing species were analyzed via Ion Chromatography. The ion chromatograph used a metal-free Dionex MFC-I column, with Dionex AG4A guard and AS4A analytical columns, an Eldex metering pump, a sample injector, and a conductivity detector. Samples were injected manually using a Valco 6-port valve with a 50 µL loop. A 1.8 mM $NaHCO_3$ and 1.7 mM Na_2CO_3 eluent was pumped at 2.8 mL/min to separate anions. In those conditions, the main products were sulfate, sulfite, and thiosulfate ions. Initially, sulfite is formed in abundance. However, with time, sulfate and thiosulfate ions dominate. The experiments duration depended on the oxidation half time at the given conditions.

Further, experiments at pH values of 4, 6, 8, and 10 were performed. The pH was kept constant using buffer solutions. The results can be seen in table 3.1:

Table 3.1: Molar fraction of formed products for the bisulfide oxidation experiments at different pH, 45°C [27]

pH	$Time_{1/2}$ (hours)	SO_3^{2-}	$S_2O_3^{2-}$	SO_4^{2-}
4	240	10.5%	17.1%	72.4%
6	102	13%	27.5%	59.9%
8	21	21.1%	35.5%	43.4%
10	16	37.1%	40%	22.9%

As can be seen, the products depend on the pH. Under acidic conditions, SO_4^{2-} is a predominant species. As the solution becomes more alkaline, the amount of sulfate ions decreases by roughly 3 times. Sulfite, on the other hand, tends to be more present at higher pH. Its concentrations are more than double at pH = 10 compared to pH = 4 [27].

Avrahami et al [28] suggested an oxidation pathway for hydrogen sulfide. They used solutions with concentrations of sulfide in the order of 10^{-4} M. The reactions were carried out in 500-ml Drechsel bottles thermostatted in the range 25-55°C. The supply of oxygen was kept constant, by bubbling a nitrogen-oxygen mixtures in the bottles. The analysis was carried via spectrophotometry. The volumes the reaction mixtures were usually between 200 and 250 ml. The proposed pathway is:

$$H_2S + H_2O \rightleftharpoons HS^- + H_3O^+ \tag{3.5}$$

Initially, the aqueous hydrogen sulfide, in basic conditions, decomposes into sulfide ions and hydrogen cations. Further, the first oxidation step occurs.

$$HS^- + 1.5O_2 \rightarrow H_3O^+ + SO_3^{2-} \tag{3.6}$$

Next, a further oxidation step occurs:

$$SO_3^{2-} + 0.5O_2 \rightarrow SO_4^{2-} \tag{3.7}$$

Here, sulfate was formed, the ultimate oxidation stage of sulfur. Depending on the conditions, sulfite can be oxidized to thiosulfate:

$$SO_3^{2-} + HS^- + 0.5O_2 \rightarrow S_2O_3^{2-} + OH^- \tag{3.8}$$

Thiosulfate is an intermediate compound which is formed in reaction with the unreacted HS^- at a higher pH. The sulfur has an oxidation state of 2 here. However, it can also be oxidized to sulfate through the following reaction:

$$S_2O_3^{2-} + 0.5O_2 \rightarrow SO_4^{2-} + S \tag{3.9}$$

Here, the highest oxidation state of +6 is achieved. An important aspect of the research performed by Zhang et al. [27] is the usage of a buffer solution, which

keeps the pH constant. The formation of different sulfur species depends on the acidity of the solution. If left under oxidative conditions without a pH regulator, the surplus of hydrogen cations would cause the pH to drop to lower levels, which would be hazardous to the equipment.

A. T. Kuhn et al describe the formation of an additional component in the hydrogen sulfide oxidation pathway [29]. Sulfur has an oxidation states of -2. In an aqueous solution, the sulfur ions can interact with each other and form chains of polysulfides, according to the following mechanism:

$$S^{-2} + nS \rightarrow S_{n+1}^{2-} \tag{3.10}$$

Polysulfides can constitute chains of different lengths. They are typically challenging to analyze. Polysulfides are not formed in conditions of oxygen excess or at higher pH and temperature values. They are regarded as a product of incomplete oxidation.

3.5 Sulfur. Chemistry and Reaction Products

Sulfur is a nonmetallic chemical element, with the atomic number of 16. In its pure form is odorless, tasteless and of yellow color. At room temperature it is a yellow solid, taking a crystalline structure. It is regarded as one of the most reactive elements. Sulfur can have many oxidation states, the main ones being -2, 0, +2, +4 and +6. It is found in water and the earth crust in the form of different minerals, usually sulfates (SO_4^{2-}) - calcium sulfate ($CaSO_4$) or barium sulfate ($BaSO_4$) of sulfides (S^{2-}) - pyrite (FeS_2) or galena (PbS). Sulfur is also found largely in underground hydrocarbon reservoirs, as mentioned in the previous chapters [30].

As a result of sulfur's reactivity, it is one of the elements which exhibits catenation, second only to carbon. This mean that sulfur atoms can group together in chains. The element forms more than 30 allotropes, being a leader in this category. Starting from S_2 (Disulfur) and up to cyclosulfurs, with the general formula S_n, where n can vary from 8 to 20 [30]. Below, the most common form of sulfur - the cyclo-octasulfur can be seen:

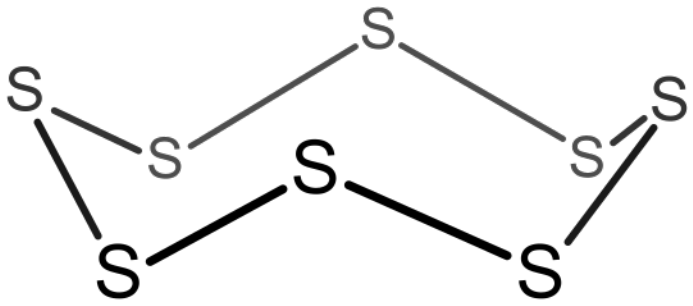

Figure 3.2: Cyclo-octasulfur structural formula

Similarly to this molecule, the sulfur ions in alkaline solutions can also group together. In their research, Fiponne et al [31] have described the formation of polysulfides in alkaline conditions. Polysulfides are large compounds consisting from sulfur ions. The number of ions in the polysulfide chain can be influenced by various factors, such as pH or temperature. A general equation for describing the equilibrium between the polysulfide ions in an aqueous solution is as follows:

$$S_n^{2-} + HS^- + OH^- \rightleftarrows S_x^{2-} + S_y^{2-} + H_2O \tag{3.11}$$

where x + y = n + 1. In alkaline conditions, the S_2^{2-} ions prevail. With increasing acidity, the chains become larger up to 5 S. At basic conditions, polysulfides can also decompose into thiosulfate ions (

$$S_x^{2-} + OH^- \rightleftarrows S_2O_3^{2-} + HS^- + H_2O \tag{3.12}$$

Polysulfides tend to be thermally unstable, converting into sulfide and thiosulfate ions. In their research, the authors have also done experiments monitoring the thermal degradation of polysulfides, at temperature ranging 95-170$^\circ C$ for 2 hours. This process begins with an OH^- ion attacking a polysulfide ion, leading to the formation of sulfide, sulfur and thiosulfate. The decomposition rate increases with higher temperature, alkalinity, and sulfur ratio in oxidation state S(0) to S(-2)[31].

The degradation rates (k) were determined using a first-order reaction, and activation energies (ranging from 45.9 to 13.0 kJ/mol) were calculated from an Arrhenius plot. Smaller polysulfide ions had higher activation energies, with S_2^{2-} and S_3^{2-} being the most stable, while S_6^{2-} was the least[31].

Decomposition rates rose with temperature; for instance, the disulfide degradation rate constant tripled from $5.42 \cdot 10^2 s^{-1}$ at 145 $^\circ C$ to $18.6 \cdot 10^2 s^{-1}$ at 170 $^\circ C$. At higher temperatures, most polysulfides convert to thiosulfate and hydrogen sulfide[31].

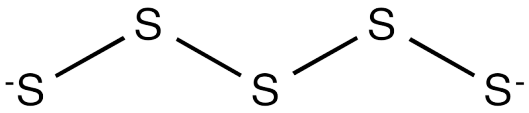

Figure 3.3: Polysulfide ion with 5 Sulfurs

The figure above displays a polysulfide ion with 5 S atoms. The degradation of larger ions occurs faster and more spontaneous, with lower activation energies. Smaller ions, moslty with 2 and 3 S tend to be more stable [31].

Chapter 4

Analytical techniques for quantification of Sulfur in various forms

The analysis of ionic solutions differs from that of neutral compounds because ions have a charge. Several techniques are available for analyzing and quantifying ions in aqueous solutions.

4.1 Ion Chromatography

Chromatography is a term in analytical chemistry that encompasses a variety of analytical techniques which are all based on separation. The latter implies the dispersal of the analyzed solution into a mobile and stationary phase. The mobile phases can be liquid or gaseous, while the stationary phases are usually solid or liquid. Some examples of stationary phases include activated carbon. For mobile phases it can be an inert gas like Argon or a liquid like hexane or water [32].

The first types of chromatography included Liquid Solid Chromatography and Thin Layer Chromatography. Later, more modern techniques were developed, like the Gas Chromatography (GC) or High Performance Liquid Chromatography (HPLC). Those techniques revolutionized the field of analytical chemistry.

Another important development was Ion Chromatography (IC). It allows the separation of ions based on the conductivity of the ionic species. There are 3 main techniques for separation of ions in aqueous phase:

- **High Performance Ion Chromatography** - In this methods, ion exchange occurs between the mobile phase and the ion exchange groups which are part of the support material. The latter usually consists of polystyrene, ethylvinylbenzene or other resins with co-polymerized ion-exchange groups. The solid stationary usually retains the targeted molecules via ionic interactions.

- **High Performance Ion Exclusion Chromatography** - Here, the separation is governed by exclusion principles, like Donnan or steric. This technique is particularly useful for the separation of weak acids from the dissociated ones.
- **Ion-Pair Chromatography** - The principle of this method is adsorbtion. A low-polarity neutral resin with large surface area is used for separation.

The two main types of ion chromatography are anion and cation exchange chromatographies. The mobile phase in ion chromatography is usually of the same charge as the ions it is able to analyze. Hence, in anion exchange chromatography the mobile phase is negatively charged[33].

The main advantages of this technique include the predictability of the effluent. The same cations always come out at the same time. In addition, in the separation technique only one interaction is involved, which increases the lasting effect of the column[33]..

Ion-exchange chromatography separates molecules on the basis of charge via electrostatic interactions with a stationary phase containing charged functional groups. The separated phases come out of the separation column at different times. The time when the targeted molecules is detected is the retention time. Analyte ions compete with exchangeable counterions for binding to these immobilized charges. Weakly bound molecules elute first, while stronger interactions require adjustments in pH or counterion concentration to disrupt binding. Elution can be done gradually (gradient elution) or in steps (step elution). The method is classified into cation-exchange (binding positively charged molecules) and anion-exchange (binding negatively charged molecules) chromatography [33].

In cation exchange, the positively charge particles are retained:

$$R - X^- C^+ + M^+ B^- \leftrightarrows R - X^- M^+ + C^+ + B^- \tag{4.1}$$

Where R-X is the matrix, M is the targeted cation, B is the anion species and C is the cation to be exchanged. In cation exchange, the positive ions are the ones to be retained. In anion exchange, the opposite case occurs.

Before ion-exchange chromatography begins, the stationary phase must be equilibrated with a buffer to establish the desired conditions. Charged ions in the stationary phase initially pair with exchangeable ions like Cl^- or Na^+. A suitable buffer is chosen to allow the targeted molecule to bind. During the washing phase, impurities that do not interact with the matrix are removed, while the targeted molecule remains bound. Elution is then performed by gradually increasing salt concentration, causing salt ions to compete for binding sites. Molecules with lower net charge elute first, while those with higher charge require stronger ionic conditions to be released [33].

A typical chromatogram consists of a horizontal axis with retention times and a vertical axis with intensity signals. There are several time points to be mentioned.

First, the column dead time (t_m) represents the times necessary for non-retained coponents to pass through the column. Then, there is the solute retention time (t_r), which is the time in which components do not travel through the column. Both summarized make up the gross retention time (t_{rm}). A schematic representation of a chromatogram of 3 targeted components can be seen in the figure 4.1 below:

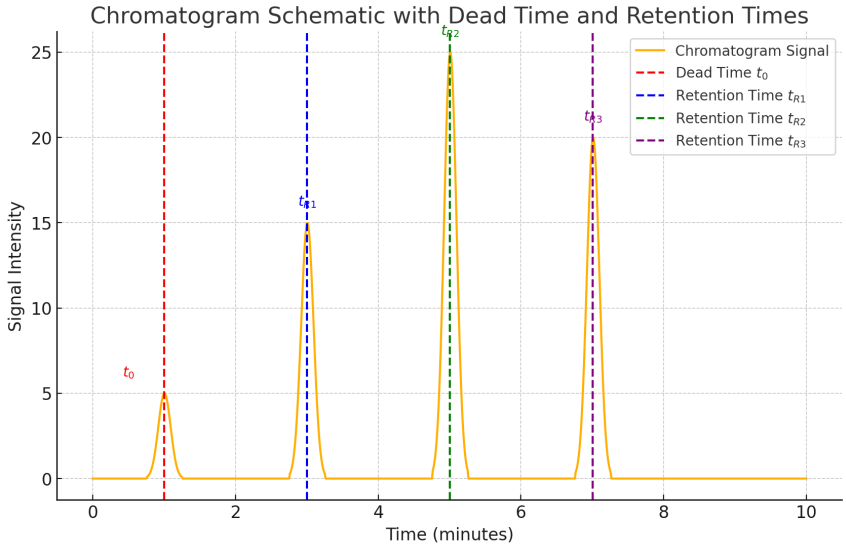

Figure 4.1: Schematic representation of chromatogram with peaks representing 3 compounds [33]

Ideally, the peak should take a Gaussian form, with its height at any position to be given by the following equation:

$$y = \frac{1}{\sigma \cdot \sqrt{2\pi}} \cdot e^{-\frac{(x-y)^2}{2\sigma^2}} \cdot Y_0 \tag{4.2}$$

Where σ is the standard deviation, y is the peak height (h) at maximum, x is a any random point on the peak. However, in most cases peaks are not ideal, as the retention process and the column do not operate perfectly. Therefore, in a practical world, most peak are with a small degree of asymmetry.

For a successful analysis, a good calibration curve is initially made. The main criteria for assessing a calibration is the R^2 - the coefficient of determination. Then a standard is run every time for method validation. When the eluent is changed, a new calibration curve could be necessary to be made.

4.2 Raman Spectroscopy

Raman Spectroscopy is an analytical technique used for determinig vibrational modes of molecules. It can be used for providing both a qualitative and quanti-

tative analysis of the solution. Raman Spectroscopy relies on inelastic light scattering where the samples is excited by photons. The latter, upon interacting with the sample scatters either elastically or inelastically. During elastic scattering, the frequency of the incoming photon does not change and no data about the molecule structure can be obtained. On the other hand, inelastic scattering can cause a gain or loss of energy by the photon. The total amount of energy must be constant, so the photon can shift to a new energy level. If the final stage is higher than the initial one, the photon is shifted to a lower frequency level - being called Stokes shifts. The opposite is called the anti-Stokes shift. A representation of the energy levels can be seen below in figure 4.2:

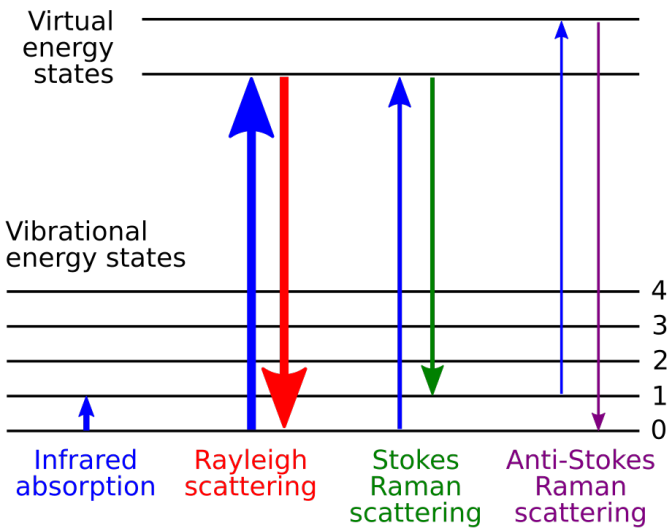

Figure 4.2: Energy level diagram for states involved in Raman spectra [34]

A more graphical representation can be seen in figure 4.3. As mentioned previously, stokes scattering caused the scattered radiation to increases its wavelength, while the anti-stokes had an opposite effect.

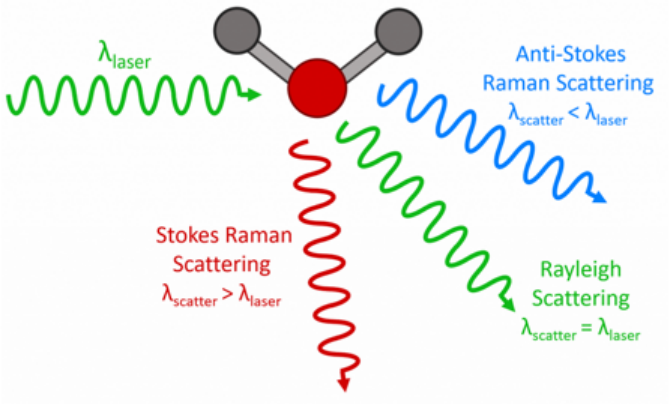

Figure 4.3: Types of Scattering in Raman [34]

Upon the interaction of a laser beam with a molecule, a dipole moment is created, with the positive and negative charges migrating towards the charges opposing their own. This is due to the charge separation cause by the electrical field. This separation of charges creates an induced dipole moment (μ) that is directly proportional to the electric field strength (E). The proportion is adjusted by the polarizability (α):

$$\mu = \alpha \cdot E \tag{4.3}$$

Raman spectroscopy detects molecular vibrations only if the molecule's polarizability changes during its motion. Consequently, a vibration is considered Raman-active when the polarizability changes at a nonzero rate with the vibration. For example, in the symmetric stretching vibration of a molecule, where atoms move in opposite directions as bonds contract or expand relative to the central atom, the electron cloud size increases, rendering the vibration Raman-active.

Raman spectroscopy has become an increasingly valuable analytical tool in various fields as a result of technological developments and its diverse applications. It is often used in biomedical diagnostics to detect cancerous tissues, DNA sequencing, and distinguish between normal and malignant cells. The technique also plays an important role in the pharmaceutical industry, assisting with the identification of counterfeit medicines and the rapid detection of illegal drugs. In the field of cultural heritage, Raman spectroscopy provides a non-destructive method for analyzing pigments in ancient artifacts and manuscripts. Additionally, it is applied in environmental monitoring to detect pollutants and in industrial processes to monitor chemical components. Forensic and security applications also benefit from Raman spectroscopy in identifying hazardous substances and explosives [35].

Main parameters in Raman Spectroscopy are:

- Integration time - defines the time in which the detector collects light. Longer

times ensure stronger signals, but if the time is too long then the detector can get saturated and impair the results.

- Laser Power - is the output of the laser, measured in mW (usual range 10 - 500 mW). For a more concentrated sample, a lower output is desired. When the concentration is high, less power gives a good performance.
- Number of spectra - The instrument usually takes several spectra and makes an average. More spectra give a more precise final spectrum. However, they also take more time to take.

One of the main advantages of Raman spectroscopy is its high sensitivity, which allows the detection of molecules at lower concentration (10^{-3}M). The technique is non-destructive and does not require extensive sample preparation, which makes it suitable for biological and cultural samples. Unlike infrared spectroscopy, Raman measurements are not significantly affected by water, which is particularly useful in biological applications. The development of portable Raman devices further enhances its utility for onsite analysis [35].

However, the technique has some disadvantages. Fluorescence interference from certain samples can obscure Raman signals, especially in biological materials. Additionally, normal Raman scattering produces weak signals, requiring enhancement techniques such as SERS (surface-enhanced Raman spectroscopy). Instruments can be expensive, and data analysis requires effort. highly qualified expert in the field [35].

Raman spectroscopy shows great potential for quantitative analysis. SERS enables the detection and quantification of trace amounts of biomolecules, drugs, and pollutants. By preparing standards of the targeted compound, a calibration curve can be made and further used for determining precise concentrations [35].

Overall, the advancements in Raman spectroscopy have significantly expanded its applications, making it a powerful tool for both qualitative and quantitative analysis across various scientific disciplines.

4.3 Inductively coupled plasma optical emission spectroscopy (ICP-OES)

Inductively Coupled Plasma Optical Emission Spectroscopy is an analytical technique used to detect chemical elements in small concentrations in aqueous solutions. This method, based on emission spectroscopy, uses inductively coupled plasma to excite atoms and ions, which emit electromagnetic radiation at wavelengths specific to each element. The plasma, typically composed of ionized argon gas, serves as a high-temperature source sustained by inductive coupling from electrical coils operating at megahertz frequencies. With temperatures within the

5500 and 9500 °C range, the plasma allows the detection of elements by measuring the intensity of light emitted at different wavelengths, which corresponds to the concentration of elements in the sample [36].

ICP-AES consists of two main components: the inductively coupled plasma (ICP) and the optical spectrometer. The ICP torch, made of three concentric quartz tubes, is surrounded by an radio frequency (RF) coil that sustains the plasma, typically using argon gas. A high-frequency electromagnetic field ionizes the argon, generating a stable plasma at around 7000 K [36].

A peristaltic pump introduces the sample into the plasma as a mist, where it is atomized, ionized, and emits element-specific radiation. The emitted light is then directed to the optical spectrometer, where it is separated into its component wavelengths. Detection is performed using photomultiplier tubes or semiconductor arrays such as Charged Coupled Devices (CCDs), enabling simultaneous multielement analysis [36].

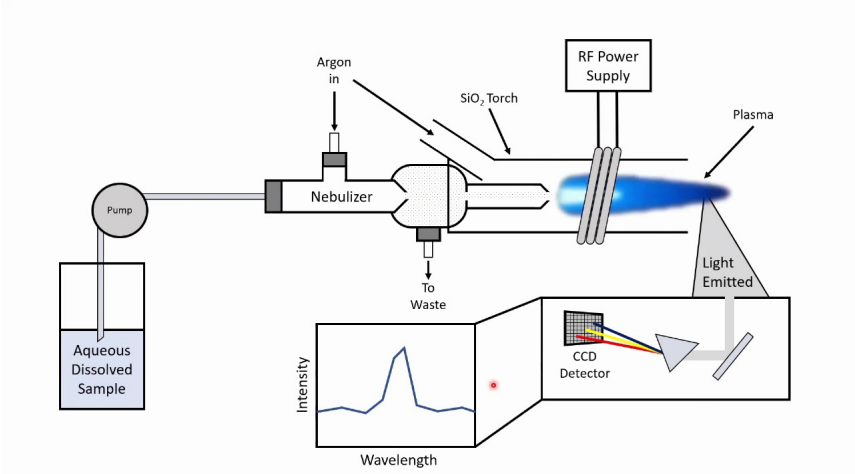

Figure 4.4: Schematic representation of a ICP AES instrument [36]

Some designs use shear gas or optical interfaces to manage plasma interaction, while detector arrays allow rapid analysis of multiple elements. The system calculates element concentrations by comparing emission intensities to calibrated reference data, with software correcting for interferences.

ICP EAS is used for detecting heavy metals in wines or drinking water. It can be used for analyzing motor oils, which helps determining which parts of the engine have integrity issues. It can be also used to determine the total Sulfur content of a sample.

Chapter 5

Project Delineation and Problem Formulation

The problem of hydrogen sulfide in the oil and gas industry has been discussed so far. It is a toxic gas with corrosive properties toward pipes and vessels and is harmful when released in the environment. Due to aging of hydrocarbon reservoirs, the problem of H_2S becomes more and more of a concern. The current use of scavengers solves the hydrogen sulfide problem, which is critical for the gas exports, which have to correspond to the industry safety standards regarding H_2S concentrations. The scavengers are also fast in removing the sulfide. Their kinetics are, however, largely unknown, which results in their excessive usage. This adds to the environmental issues related with the release of scavengers into the sea. It is harmful to aqueous life, and the release of large amount of unreacted scavengers only enhances the issue. Hence, alternatives to the classical scavengers are to be sought.

In this project, the possibility of avoiding the use of scavengers is researched. Instead of disposing spent and unspent scavengers in the sea, the usage of a solvent to absorb H_2S is investigated. The absorption of H_2S and its further oxidation limits the environmental impact of the process. In its highest oxidation form, sulfur can be found in the form of sulfate. Those ions are not harmful to aquatic life, as they naturally found in water. The absorption, however takes longer time and it has been little researched.

Some solvents that proved effective in capturing hydrogen sulfide are amines and sodium hydroxide (NaOH). Previous researches provide a general idea about what products to expect after the oxidation. However, the lack of research in hydrothermal oxidation of the bisulfide ion provides motivation for analyzing in detail the obtained products and the pH of the oxidized solution. Hence, the project question:

What reaction conditions in hydrothermal oxidation of (H_2S) provide a better sulfide conversion into sulfate SO_4^{2-} and what are the intermediate products at different reaction conditions?

The experiments will be performed on sodium sulfide solutions, as this would be the product of absorbing sulfide with sodium hydroxide. In this project, the experimental work will focus on hydrothermal oxidation and analysis of the samples. The goals of the research are to determine optimal reaction conditions for oxidizing the bisulfide ion, as well as to determine the reaction components and to assess how suitable a solvent would potentially be for such purposes.

Chapter 6

Materials and Experimental Methods

The previous chapters laid a theoretical understanding of the topic. Here, the gained knowledge will be applied in different experiments and analysis.

Some preliminary trials were performed to understand how the setup works and also to obtain an idea about the magnitude of obtained results. Also, those runs had the role to eliminate some safety concerns.

6.1 Reagents and Equipment

6.1.1 Chemicals used

Several compounds were used in the experimental work. Sodium sulfide (Na_2S, CAS 1313-84-4, >99%), purschased from Sigma Aldrich was used for simulating the products of scavenging H_2S by NaOH. The compounds were available in the form of trihydrate ($Na_2S \cdot \sim 3H_2O$). The exact water content was determined using Karl Fischer titration. Acetonitrile was used as an internal standard for the Raman Spectroscopy analysis. It was purchased from Sigma Aldridch (CH_3CN, CAS 75-05-8, >99%). Sodium sulfate (Na_2SO_4, CAS 7757-82-6, >99%) and Sodium thiosulfate ($Na_2S_2O_3$, CAS 7772-98-7) were also used in Raman Spectroscopy calibration for the analysis of reaction products. The oxygen for the oxidation was provided as technical air (21% O_2, 79% N_2, purchased from Air Liquide).

6.1.2 High Temperature Reactor

The hydrothermal oxidation experiments were executed using a customized hight pressure hight temperature (HPHT) reactor made by SITEC-Sieber Engineering

AG, Switzerland. The hydrothermal oxidation experiments were performed with the help of Alessandro Perrucci, PhD Fellow at Aalborg University in Esbjerg.

Setup description

The central component of the setup is the reactor (R1, 99 mL), capable of operating at temperatures up to 400°C and pressures up to 300 bar. A schematic representation of the setup can be seen in the figure 6.1.

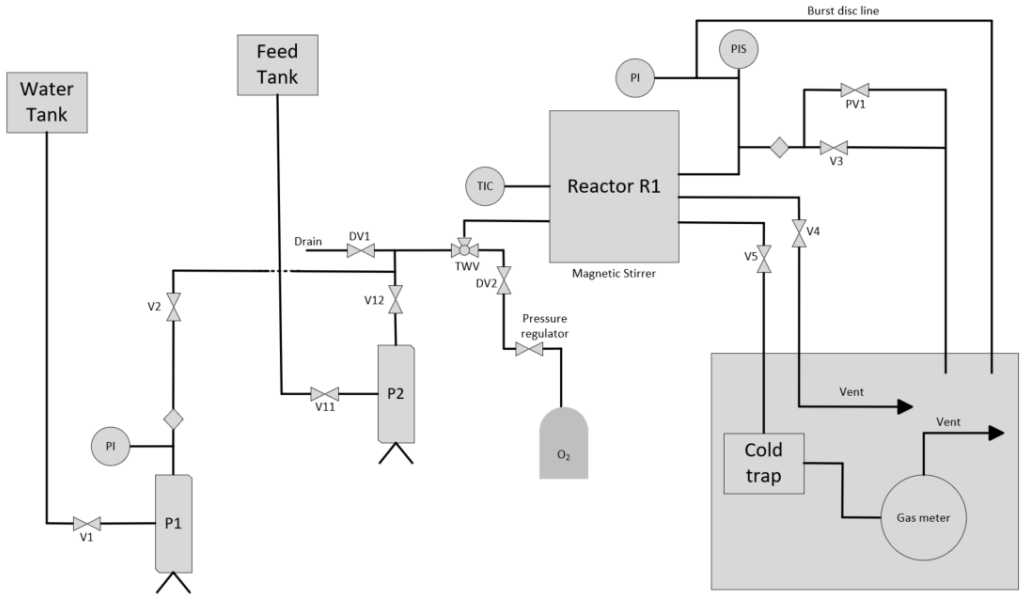

Figure 6.1: Schematic diagram of the setup

Heating is achieved via four 500 W electrical cartridges embedded in the reactor shell, managed through a combined cascade/slave PID control system. A type K thermocouple (class 1, accuracy ± 0.5%), measures the temperature inside the reactor. Reactor pressure is monitored at the top connection with a gauge accurate to ± 1%. A magnetic stirrer with a heating plate is installed at the bottom of the reactor. It helps improve the mass transfer by mixing the contents and reduce the heat loss from the bottom of the reactor. The reactor is surrounded by a high temperature jacket, acting as an insulator.

Figure 6.2: Front part of the reactor

Figure 6.3: Back part of the reactor

The system includes two high-pressure precision hand pumps (P1 and P2) with a stroke volume of 100 mL, delivering 2 mL per revolution and supporting a maximum pressure of 300 bar. Pump P1 is used to inject or withdraw water for precise pressure adjustments and is protected by a filter (F1) to prevent contact with slurry particles. Pump P2 is specifically designed with a protective seal, allowing it to handle various feeds. The pressure at the discharge of both pumps is measured by dedicated pressure gauges.

The setup also features a flushing line to recover any slurry residues not introduced into the reactor. The total dead space volume in the system is 5.9 ml. The pressure of the system is limited by a pneumatic valve and a rupture disc set to release at 350 bar. Two sampling ports (for liquid and gas phase), positioned at the top and bottom of the reactor, enable the withdrawal of reactor contents. The bottom port is directed via a pipe, through a condenser to a collection flask, which is placed in a bucket with ice to prevent its evaporation.

Procedure

For hydrothermal oxidation to occur, an aqueous solution of the feed and an oxidant are needed, in this case the oxygen contained in the technial air cyllinder. For the experiment, solutions of 100-200 millimolar of sodium sulfide (Na_2S) were prepared - those were the feed. The flasks were weighted before and after they were filled with sample, to know exactly how much ended up in the reactor. The same was done for water, with 20-30 grams ending in the reactor. Oxygen was introduced in 2 excess levels at 140% and 200%, after the reactor was sealed. The excess was calculated on a molar basis. After the water was poured, the available volume in the reactor by subtracting the water from the total volume. The empty

reactor has a volume of 99 ml, but considering the piping around it, the volume accounted for is 103, also used in previous projects [37]. This serves as basis for calculating the required pressure to account for desired excess of oxygen. Depending on the feed volume and oxygen excess, the air pressure in the reactor ranged from 8 to 39 bar. The necessity for excess moles of oxygen is converted into mass. Knowing both the mass and volume, the density can be determined from the NIST website [38]. Later, the required pressure for achieving the targeted density at a specific temperature is obtained. In parallel, a sodium sulfide solution was poured into the feed tank.

After the reactor is pressurized with air, the heating is turned on. In this experiment, temperatures were ranged from 150 to 300$^{\circ}C$. When the heating is complete, the feed is injected in the reactor from the feed tank. This is done using the pump P, which injects directly into the reactor. The injections are done slowly, with a rate of around 20 ml/min. When the final amount is injected, the timer is started. Reaction times range from 1 to 20 minutes. The start time (t=0) is when the feed is poured in the reactor and mixed with the water present there. When the reaction is finished, the products are ejected into the cold trap and then, after cooling, retrieved from the collection flask - this marks the end time. The flask is weighted before and after the effluent is ejected into it. After all the liquids which remained in the reactor are weighted for the mass balance, the oxidation products are brought for analysis.

It is to mention that due to previous experiments performed on this reactor with H_2S scavengers, the samples effluent was of a dark color. An example can be seen below in figure 6.4

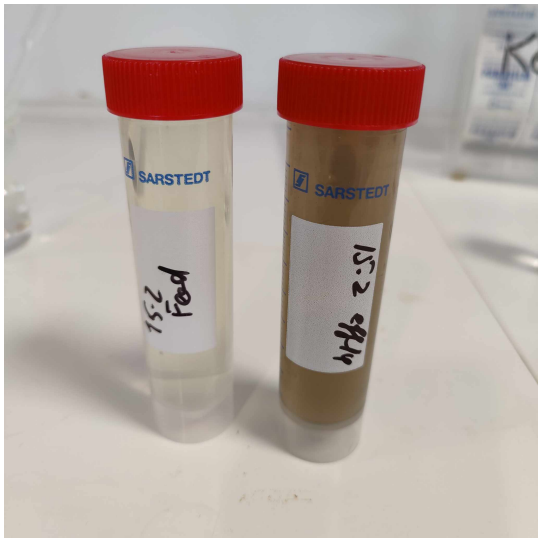

Figure 6.4: The feed and the effluent from an experiment

The dark pigment from the effluent vial precipitated after some time. Later, it was analyzed to determined whether it contained some sulfur.

6.2 Analytical equipment

The analysis of the samples was performed via Raman Spectroscopy, Sulfite Analysis kit and Ion Chromatography (IC).

6.2.1 Water Content

Sodium Sulfide (Na_2S) was used as source of bisulfide solution. Sodium Sulfide was in a trihydrate mixture. For a more precise result, Karl-Fischer titration was employed. Sodium Sulfide trihydrate (Na_2S was grinded into powder and then around 1 grams of samples was placed inside the apparatus. During the process, the temperature rises up to $210°C$, so that all the water evaporates. Then, the water goes into the titration chamber, where its precise amount is determined. In the end, the water content of the sample is displayed. 3 repetitions were made to eliminate random error and the average was used further.

In the end, the water content was determined to be 41%. This was used to calculate the sulfur balance.

6.2.2 Raman Spectroscopy

The Raman Spectrometer from MarqMetrix was used. The laser excitation wavelength is 785 nm. The spectral range is from 100 to 3250 nm^{-1}. For the analysis, an integration time of 10 000 ms was used, with 6 spectral averages and 400 mW of laser power. Below, a picture of the setup with a vial inside can be seen in figure 6.5.

Figure 6.5: The Raman probe in the cell

The samples were placed in a glass vial for analysis. The vials were placed in a dark box to avoid interference with external light sources. Approximately 5 ml of liquid ended up in the vials, of which 2.5 ml came from the reactor effluent and 2.5 was an internal standard solution of acetonitrile, 400 mM, prepared in advance.

After the spectra collection, they were analyzed. This was performed by Sergey Kucheryavskiy, Associate Professor at Aalborg University in Esbjerg. The spectra obtained from the Raman were further normalized, and their baseline was corrected, so an adequate quantitative comparison between the samples can be performed. It is important to mention that both the effluent and the feed samples were analyzed using Raman, so clear qualitative data about the input and output of the system can be generated for further assessment. The targeted wavelength were for the chemical bonds between H and S, whose vibrations occur at the wavenumber 2590 cm^{-1} and between S and O, which occur at

Initially, calibration curves were made for all of the potential oxidation products, such as bisulfide (HS^-), sulfate (SO_4^{2-}), sulfite (SO_3^{2-})and thiosulfate ($S_2O_3^{2-}$). Later, however, some peak overlapping was discovered during the analysis of the

last 3 components, making it hard to differentiate between some of them. Therefore, it was decided to use Raman only for bisulfide. Also, other methods have been identified for the rest of the components.

For determining the bisulfide concentrations, calibrations were made. For that, solutions with concentrations of 0, 5, 10, 20, 30, 40 and 50 mM were prepared. All solutions were made in triplicates. The samples were diluted with a 100 mM acetonitrile solution, as an internal standard. The feed was also diluted with acetonitrile. Additionally, due to the color of some samples, the feed was additionally diluted with water to obtain a more clear solution.

The raw taken spectra was normalized and baseline correction techniques were applied. In the image below, the raw and processed spectra can be seen:

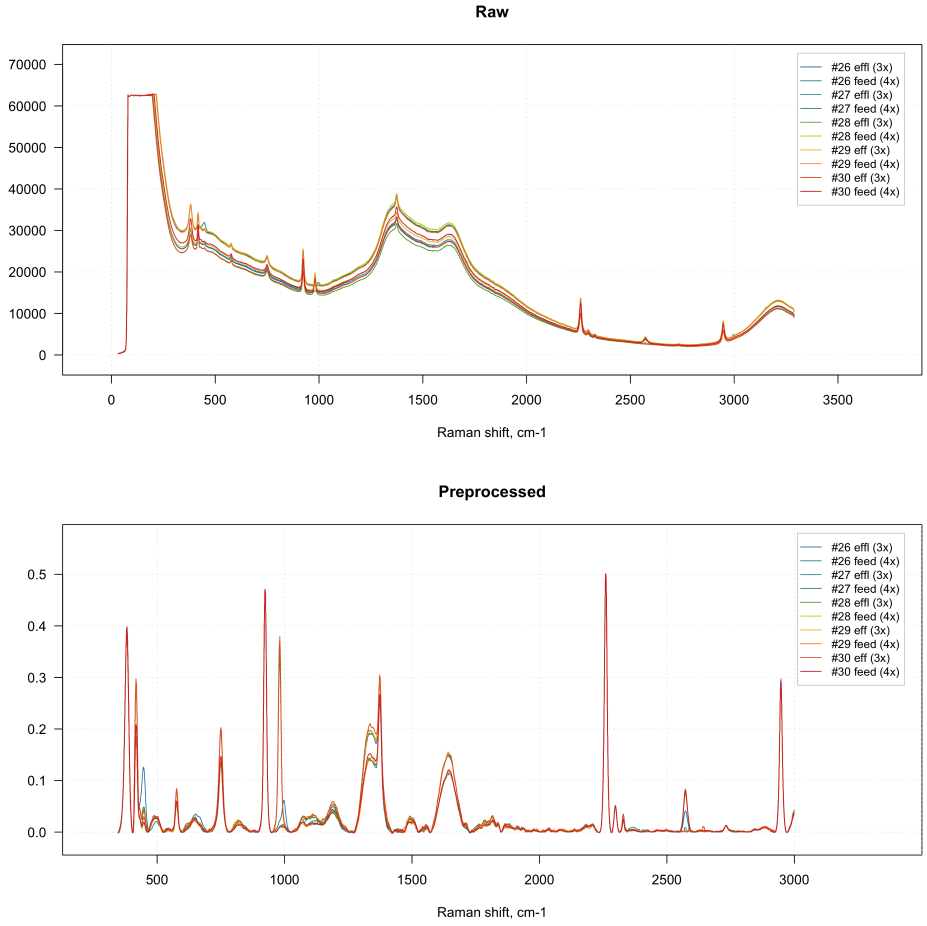

Figure 6.6: Raw vs Processed Spectra

After the spectra was processed, the bisulfide had been quantified based on the internal standard and on the calibration curves. The spectra of the bisulfide (HS^-)

can be seen in figure 6.7

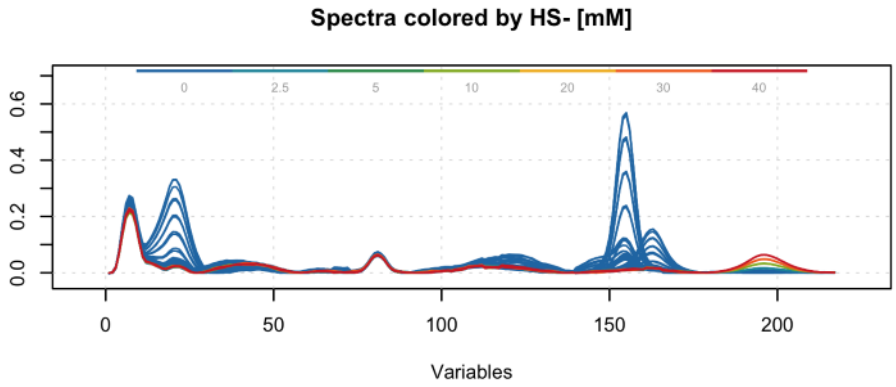

Figure 6.7: The spectra of the bisulfide ion

The calibration results were used by Sergey Kucheryavskiy to quantify the bisulfide.

6.2.3 Ion Chromatography

The IC used in this project was from Eco IC. The setup consist from a high pressure pump for the eluent (8 mM solution of Na_2CO_3), an inline filter with 2 μm pore size, which retains potential contaminants from the eluent. There is also an injection valve, a rotor for samples and a peristaltic pump for pumping the sample. The analysis is done by the conductivity detector, which measures the conductivity of the solution coming out of the separation column.

In this research, it was attempted to quantify sulfite (SO_3^{2-}), thiosulfate ($S_2O_3^{2-}$) and sulfate (SO_4^{2-}) with the IC. To determine the possibility of doing that, solutions of sulfite, thiosulfate and sulfate with the concentrations of 10 mg/l were made. The sulfite ions had retention times similar to those of the sulfate ones. Therefore, their quantification by this IC was deemed impossible. Further, alternatives for the sulfite analysis were sought.

In the case of thiosulfate, different results were obtained. Initially, the peak could not be observed on the chromatogram. Later, the ejection time was increased from 12 to 20 minutes. Around 14-15 minutes, a new peak was noticed. The hypothesis was that is is thiosulfate. To confirm this, a mixture of sulfate and thiosulfate was made. The new chromatograms showed both peaks again. After confirmation that the thiosulfate ion can be seen, a calibration curve for the compounds was made, in the range of 2-20 mg/l, which is the practiced range for sulfates. Solutions of 2, 5, 10 and 20 mg/l were prepared. In the figure 6.8 below, the peaks for sulfate and thiosulfate can be seen:

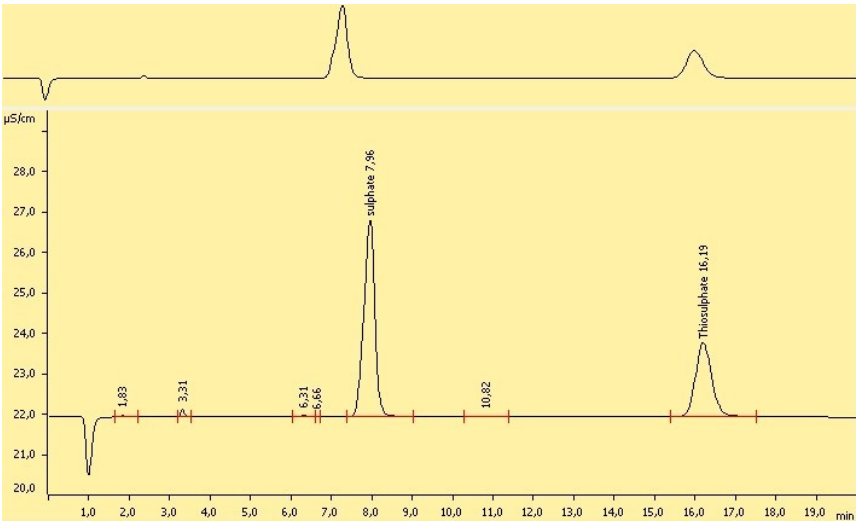

Figure 6.8: Chromatogram from the IC

The standards were 2, 5, 10 and 20 mg/l. The calibration was done in doubles for each standard. The diluted samples were analyzed and the results converted to grams of pure sulfur for comparison.

The calibration curves were made for sulfate and thiosulfate.

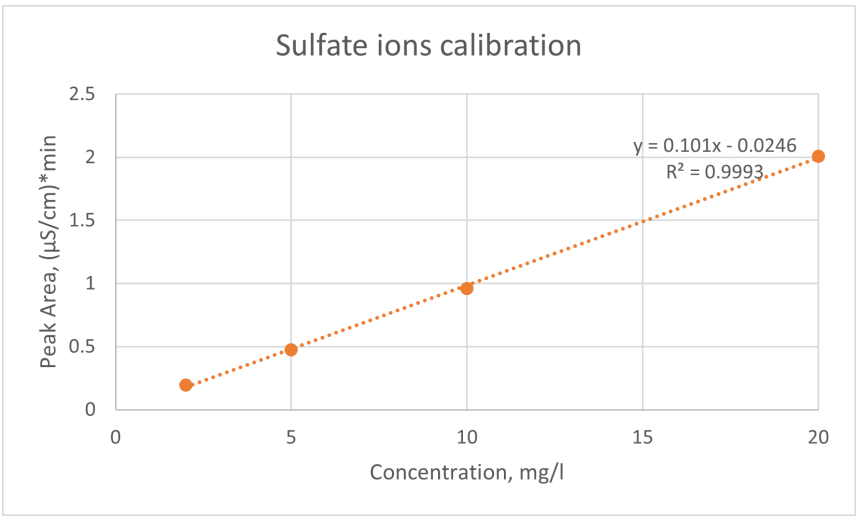

Figure 6.9: Sulfate calibration

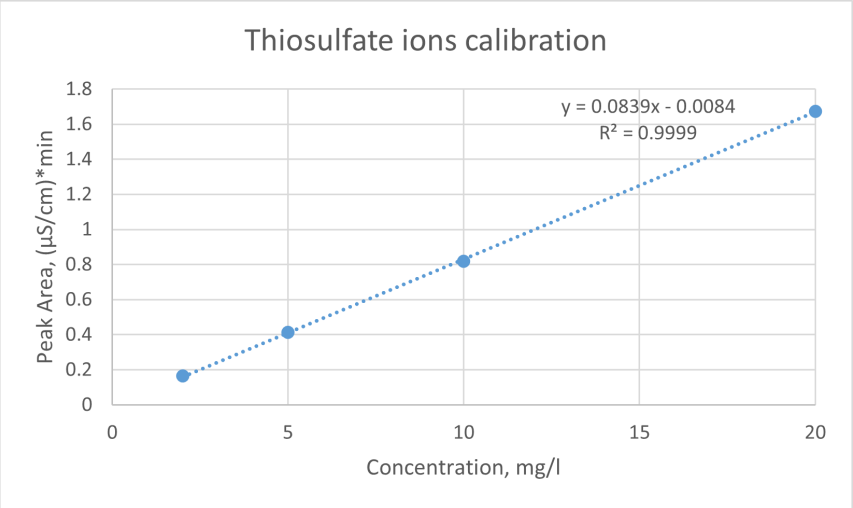

Figure 6.10: Thiosulfate calibration

The samples were diluted 100 to 500 times, depending on concentrations, and then analyzed on the IC. The peak area obtained was input into the curve, and the concentration was obtained.

6.2.4 Analysis kit for SO_3^{2-}

The analysis of SO_3^{2-} ions was performed via a Spectroquant Sulfite test cell kit. The kit consits of 25 reaction cells and one bottle of reagent (2,2′-dinitro-5,5′-dithiodibenzoic acid). In pH conditions of 4-9, sulfite ions react with 2,2′-dinitro-5,5′-dithiodibenzoic acid (Ellman's reagent) to form an organic thiosulfate, resulting in the release of a thiol, which turn the solution into yellow. The intensity of the yellow color is linked to the SO_3 concentration. The cell is inserted in a spectroquant, where the sample is recognized by the QR code on the vial and the concentration is shown on the screen. An image of the used kit can be seen below:

Figure 6.11: The used sulfite kit

The kit was tested with a standard solution of 10 mg/l of SO_4^{2-}, SO_3^{2-} and $S_2O_3^{2-}$ to determine its performance and selectivity among similar sulfur-containing ions. The kit proved to be effective in distinguishing the sulfite from the 2 other ions, giving the correct result, with an error of around 10%. Therefore, the kit was used for SO_3^{2-} quantification, while the SO_4^{2-} was quantified by subtracting the sulfite concentration obtained by the kit from the IC data regarding sulfate, but which interferes with sulfite.

6.2.5 Total Sulfur Content (ICP OES)

Induced Coupled Plasma Optical Emission Spectroscopy was employed for the determination of the total sulfur content of the samples. The used ICP OES is manufactured by Perkin Elmer, model Optima 8000. The plasm is argon based. The RF power is 1500 W and a cyclonic nebulizer was used. The plasma flow rate was 12 l/min, for the auxiliary gas it was 0.2 l/min, and for the sample it was 1 l/min. The sulfur was analyzed at 181.975 nm.

For this experiment, 2 different effluent samples were taken for analysis. The hypothesis was that the dark sediment might contain sulfur. Therefore, the analysis was performed on both the transparent part of the sample (when the sediment is

settled at the bottom) and shaken sample. Also the feed solution was analyzed, to make a comparison between the sulfur contents before and after the oxidation (figure 6.4).

The effluent samples were diluted 100 and 200 times, while the feed was diluted 250 and 500 times. The difference is due to the effluent being already diluted by the water from the reactor. 20 ml of each solution was transferred into autoclave bottles, together with 5 ml of nitric acid (HNO_3). In the autoclave, at $140°C$ for 2 hours, the samples were digested in the presence of the nitric acid, meaning the sulfur was oxidized to its highest state of +6. After the samples cooled down, they were analyzed in the ICP. A calibration curve from 1 to 16 mg/l had been made in advance and the samples were tested. The obtained results for feed and effluent were compared.

6.2.6 Analytical techniques summary

Many analytical techniques have been employed. As a summary, in table 6.1 all of the employed techniques are presented:

Analyzed species	Analytical technique
Bisulfide ion (HS^-)	Raman Spectroscopy
Sulfite ion (SO_3^{2-})	SO_3^{2-} kit
Thiosulfate ion ($S_2O_3^{2-}$)	Ion Chromatography
Sulfate ion (SO_4^{2-})	Ion Chromatography
Total Sulfur Content	ICP-OES

Table 6.1: Analytical techniques employed

Due to the complexity of the sulfur analysis, many techniques have been used. Therefore, when summed up the obtained results are not perfect.

6.3 Results Analysis

The results were presented in various forms. The data obtained from instruments was converted to concentration of sulfur-based components in the reactor effluent or mass sulfur equivalent. The effluent was further diluted for analysis. The initial concentration of bisulfide (CH_{HS0}) is defined as the concentration in the reactor when the feed was just injected.

For the Raman Spectroscopy, the result was obtained in mM of bisulfide. Hence, it was just subtracted from the initial bisulfide concentration to obtain the functional conversion.

$$X_{HS^-} = \frac{N_{HS_0^-} - N_{HS^-}}{N_{HS_0^-}} \tag{6.1}$$

The $N_{HS_0^-}$ would be the number of moles of bisulfide injected in the reactor and the N_{HS-} of the ejected bisulfide. Due to some water already present inside, the concentration is diluted. Hence, the dilution factor is defined:

$$D_{factor} = \frac{V_{water} + V_{feed}}{V_{feed}} \tag{6.2}$$

During the experiment, the masses are taken in grams. However, due the solutions being of weak concentrations, a pure water density was assumed, which is approximately 1 g/ml at room temperature ($20^{\circ}C$). Hence, V_{water} represents the volume of water placed in the reactor from the beginning and V_{feed} represents the volume of the bisulfide solution injected in the reactor. The dilution factor represents how much was the bisulfide solution diluted in the reactor.

The results for the sulfite (SO_3^{2-}), thiosulfate ($S_2O_3^{2-}$) and sulfate (SO_4^{2-}) were obtained in mg/ml. First step, the concentrations were multiplied by the dilution. Since the IC and the sulfite analysis kit have a limit of 20 mg/l, the samples were diluted up to 500 times. For molar concentrations, the mass concentration were divide by the molar mass of the components.

In the end, the mass of pure sulfur contained in each species was calculated:

$$M_S = C_{mass} \cdot V_{effluent} \cdot M_{frac} \tag{6.3}$$

The M_S - the mass of pure sulfur contained in each of the ions is calculated by multiplying the mass concentration (C_{mass}) to the effluent volume. Thereby the mass of pure sulfite/thiosulfate/sulfate is obtained. Further, the mass fraction (M_{frac}) of sulfur in each components is determined:

$$M_{frac} = \frac{M_S}{M_{total}} \tag{6.4}$$

For example, SO_4^{2-} has a mass of 96 g/mol. It has one S atom, which weights 32 g/mol. The sulfur fraction in sulfate is therefore around 0.33.

The different obtained values were used for easier data visualization in the next results section.

6.4 Modeling of data

After the results were obtained, it was attempted to model the reaction kinetics. The reaction scheme proposed by Zhang et. al. (inspired from Avrahami et al [28]) was used as basis for the analysis of the obtained components [27]:

$$H_2S_{(aq)} \leftrightarrow HS^- + H^+ \tag{6.5}$$

$$HS^- + 1.5O_2 \rightarrow SO_3^{2-} + H^+ \tag{6.6}$$

$$SO_3^{2-} + 0.5O_2 \rightarrow SO_4^{2-} \tag{6.7}$$

$$SO_3^{2-} + HS^- + 0.5O_2 \rightarrow S_2O_3^{2-} + OH^- \tag{6.8}$$

$$S_2O_3^{2-} + 0.5O_2 \rightarrow SO_4^{2-} + S \tag{6.9}$$

However, for the modeling, a simplified version of the process was created, due to the complexity of the reaction scheme. A similar approach is adopted by Zhang et al [27], where they measured the disappearance rate of bisulfide at different pH levels. Due to the fact that initially the feed contains only bisulfide and sulfate represents the final oxidation product. Therefore, the authors simplified the the process by analyzing the consumption of HS^- as a whole. The kinetic model was inspired from Montesantos et. al [37]. The basic model for bisulfide oxidation can be described by the equation:

$$-r_{HS} = k \cdot {C_{HS}}^m \cdot {C_{O_2}}^n \tag{6.10}$$

where r_{HS}^m represents the rate of bisulfide disappearance per unit time and volume of the reacting aqueous phase. C_{HS} represents the molar based concentration of the bisulfide ion and C_{O_2} the concentration of oxygen. The exponents m and n are the orders of the reaction with respect to bisulfide concentration and oxygen. Just like in Montesantos' work, here it is assumed that the oxygen is in excess, with its transfer to the aqueous phase being much faster than its consumption. Under this assumption, the rate equation is simplified to:

$$-r_{HS} = k' \cdot {C_{HS}}^m \tag{6.11}$$

The oxygen concentration is eliminated and only the bisulfide concentration becomes relevant. The rate constant k is switched for the pseudo-constant k', which assumes oxygen saturation. Further, the integral method of analysis is used to verify different power law equations. When a suitable equation is found, it is used to determine the rate constants for 150, 200, 250 and 300$^\circ C$ and 140% oxygen excess.

Different models from the integral method for the reaction order were tried.

Zero order:

$$\frac{dC_{HS_0}}{dt} = -k' \rightarrow C_{HS} = C_{HS_0} - k't \tag{6.12}$$

First order:

$$\frac{dC_{HS_0}}{dt} = -k' \cdot C_{HS} \rightarrow ln(\frac{C_{HS}}{C_{HS_0}}) = -k't \tag{6.13}$$

1.5 order:

$$\frac{dC_{HS_0}}{dt} = -k' \cdot {C_{HS}}^{1.5} \rightarrow \frac{1}{\sqrt{C_{HS}}} - \frac{1}{\sqrt{C_{HS_0}}} = \frac{1}{2}k't \tag{6.14}$$

Second order:

$$\frac{dC_{HS_0}}{dt} = -k' \cdot {C_{HS}}^{2} \rightarrow \frac{1}{C_{HS}} - \frac{1}{C_{HS_0}} = k't \tag{6.15}$$

2.5 order:

$$\frac{dC_{HS_0}}{dt} = -k' \cdot {C_{HS}}^{2.5} \rightarrow \frac{1}{{C_{HS}}^{1.5}} - \frac{1}{{C_{HS_0}}^{1.5}} = \frac{3}{2}k't \tag{6.16}$$

Third order:

$$\frac{dC_{HS_0}}{dt} = -k' \cdot {C_{HS}}^{3} \rightarrow \frac{1}{{C_{HS}}^{2}} - \frac{1}{{C_{HS_0}}^{2}} = 2 \cdot k't \tag{6.17}$$

After each order of reaction is plotted and analyzed, the one with the best R^2 and lowest intercept is picked. According to the formula then, the rate constant k' is determined.

Chapter 7

Results and Discussion

After the experiments were performed, the samples were analyzed and the products' composition and concentration were determined.

An important step in the experiments were the initial trials, which determined some baseline for the rest of the experiments in terms of safety and operational parameters,

7.1 Performed experiments

As mentioned in the Material and Methods chapter, Na_2S trihydrate feed was subjected to Karl-Fischer titration to determine its water content. After 3 runs, an average water content of 41% was obtained. This was used further to calculate the sulfur balance.

The experiments were carried out at 1, 3, 5, 10 and 20 minutes. The temperatures were 150, 200, 250 and 300$^{\circ}C$. Two excess oxygen levels of 140 and 200% were tested. Initially, experiments al lower temperatures (150 and 200 $^{\circ}C$) were tried. This constituted a first stage of the experiments that helped determine in which direction the parameters are to be changed. A full table with all the experiments performed can be viewed in Appendix A.

7.2 First stage experiments

In the first stage of the experimental work, 5 reaction times (1, 3, 5, 10 and 20 minutes) were tried, at temperature of 150 and 200$^{\circ}C$, with a 140% molar excess of oxygen. A table with the parameters can be viewed below:

Table 7.1: First stage experiments

Experiment number	Temperature	Time	Oxygen level
2	150	5	140.00%
3	200	5	140.00%
4	150	10	140.00%
5	200	10	140.00%
7	200	1	140.00%
8	200	3	140.00%
9	200	20	140.00%
10	150	3	140.00%
11	150	20	140.00%
12	150	1	140.00%

For the first stage experiments, solutions of 100 mmol/l of Na_2S were prepared. For an 140% excess of oxygen, 8 bars of air were charged into the reactor, alongside 20 grams of water. After being heated, the system's pressure rose to 15 bar. At 15 bar and 150°C, the water density corresponds to 917 kg/m^3. The results for the 4 measured species can be seen below:

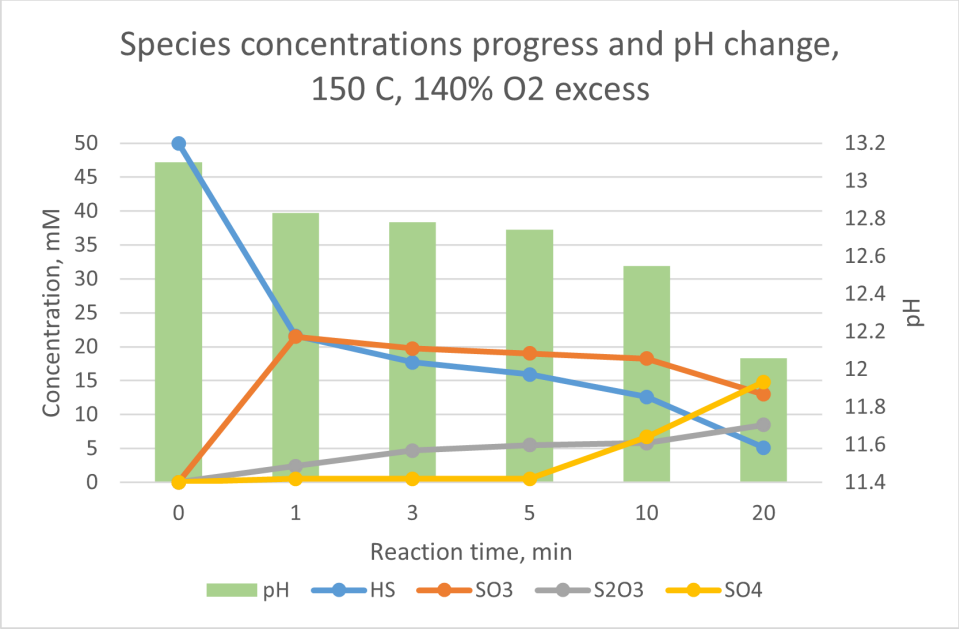

Figure 7.1: Species concentrations and pH at 150°C, P=15 bar

The results are aligned with the expectation that the sulfide concentration will decrease with time as it is converted to other species. The HS^- concentration also changes disproportionally with the reaction time. At the maximum reaction time

of 20 minutes, the bisulfide is consumed almost entirely and the oxidation process is now complete. This is reflected in the pH. The values decreased from 13.1 as the initial value to 12.1 after 20 minutes of reaction. This is reflected in the H_2S oxidation scheme from the previous chapter, where HS^- anions are consumed in the second reaction, contributing to a lower pH. Consequently, more HS^- oxidized causes more hydrogen protons to be generated, which acidify the medium.

The sulfite (SO_3) is the first of the ions to be generated. Its concentration increases initially and then decreases towards the end. Sulfite and thiosulfate are both intermediate products according to the reaction scheme. However, at 150°C the thiosulfate does not reach a downward concavity. The final products of the oxidation is considered to be the sulfate ion (SO_4). Its concentration initially stays low but starts to increase after 5 minutes. At 20 minutes, the sulfate is the most abundant species. Despite that, the full potential of the reaction is not reached, since not all sulfur ix oxidized to +6. The temperature is then increased to 200°C. The pressure at this temperature was 25 bar. At 25 bar and 200°C, the water density corresponds to 865 kg/m^3.

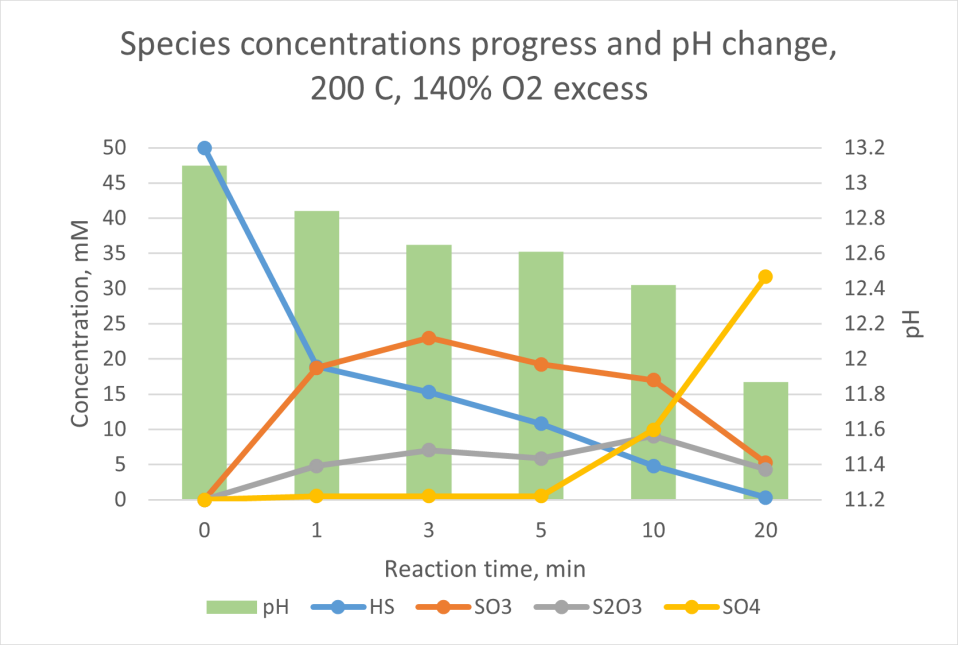

Figure 7.2: Species concentrations and pH at 200°C, P=25 bar

At 200° C, all the sulfite is consumed after 20 minutes. As in the previous case, the SO_3^{2-} ions increase initially in concentration, after which they decrease, being converted to other sulfur species. Thiosulfate $S_2O_3^{2-}$ ions start decreasing at 20 minutes, while the sulfate (SO_4^{2-}) ions increase after 5 minutes. The trends at 200°C seem similar to those at 150°C. The main difference is that in the latter

case, less sulfate was generated and the thiosulfate concentration was still growing at 20 minutes. The pH, as in the 150°C experiments, was decreasing with time, with the highest decrease noticed at 20 minutes. The lowest value here is below 12, signaling a higher pH drop, explained by a higher bisulfide conversion rate.

In the following figure, the mass-based selectivity of the reaction products can be visualized. The analyzed ions are sulfates (SO_4^{2-}), sulfites (SO_3^{2-}), thiosulfates ($S_2O_3^{2-}$) and unreacted sulfides (HS^-). The values are calculated as moles of sulfur in the form of different species and presented as percentage of the initial sulfur amount injected as feed.

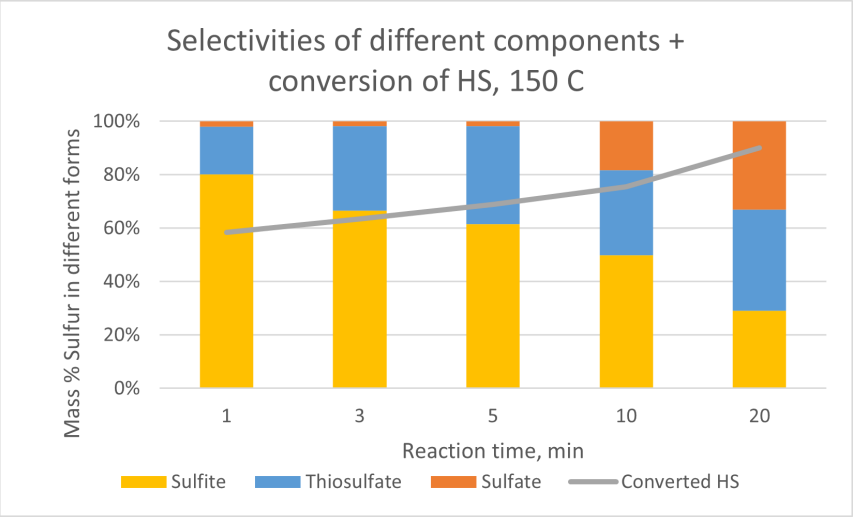

Figure 7.3: Selectivity and Sulfide conversion at 150°C

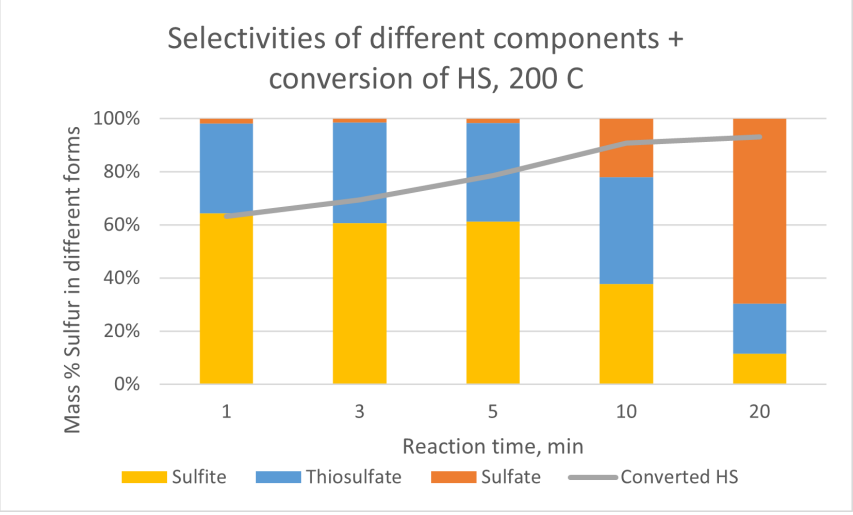

Figure 7.4: Selectivity and Sulfide conversion at 200°C

The most extreme conditions of 20 minutes and 200°C yielded the biggest amount of sulfate (SO_4^{2-}). At a reaction time of 1 minute, most of the sulfur is in form of sulfite ions. Those corresponds to the lower oxidation states of sulfur. A trend in which the oxidation state of the products increases with the reaction time can be noticed. While at 1 minute the reaction progress is not far, at 3 and 5 minutes the presence of thiosulfate becomes more noticeable. In the mass-based selectivity graphs, the thiosulfate effect is emphasized, as it contains 2 sulfur atoms.

Those 10 experiments served as a baseline and reference for the next experiments. Due to the best result being obtained at the most extreme conditions of 20 minutes and 200°C, the temperature for the next conditions has been increased. Also, different oxygen levels have been tried.

7.3 Analysis of the 2-phase effluent

As mentioned in the previous chapter, some of the effluent had a dark colored precipitate at the bottom of the vial. After the first experimental stage, the analysis of sulfite was not pursued yet, therefore the sulfur balance was not closing. The hypothesis was made that the remaining sulfur is present in the precipitate. For that, the precipitate was analyzed eith the ICP OES. Two chosen effluent samples and one feed sample were analyzed. The analysis was performed on both the homogeneous effluent (with the precipitate shaken) and the heterogeneous sample (with the precipitate at the bottom). The total sulfur content revealed around 55 mg of sulfur in the feed and around 60 mg in the effluent. Therefore, it was deemed that the sulfur is not contained in the precipitate and other forms of sulfur must be researched. This triggered the pursuit of SO_3 analysis.

7.4 Second stage experiments

After the first stage experiments, several conclusions were made. First, higher temperatures must be pursued. Second, lower reaction time of 1 and 3 minutes do not yield any significant results. Therefore, it was decided to pursue higher temperature experiments with higher reactions times of 5, 10 and 20 minutes. Also, higher levels of oxygen were tried. Due to the increased temperature, the vapor pressure value has now changed. The system's initial pressure had to be changed. Since the oxygen excess level was a parameter, it was decided to increase the bisulfide concentration. As a result, the starting pressure for the 140% oxygen excess was 27 bar and for 200% it was 39 bar. The full table with performed experiments in the second stage can be seen below:

Table 7.2: Second stage experiments

Experiment number	Temperature	Time	Oxygen level
15	250	5	140.00%
16	250	10	140.00%
17	250	20	140.00%
18	250	5	140.00%
19	250	5	140.00%
20	250	10	140.00%
21	250	20	140.00%
22	250	10	140.00%
23	250	20	140.00%
24	250	5	200.00%
25	250	5	200.00%
26	250	10	200.00%
27	250	10	200.00%
28	250	10	200.00%
29	250	20	200.00%
30	250	20	200.00%
31	250	20	200.00%
32	250	5	200.00%
33	300	5	140.00%
34	300	10	140.00%
35	300	5	200.00%
36	300	10	200.00%
37	300	5	200.00%
38	300	5	140.00%
39	300	10	200.00%
40	300	10	140.00%
41	200	20	140.00%
42	200	20	140.00%
43	200	20	200.00%
44	200	20	200.00%
45	300	20	200.00%
46	300	20	200.00%
47	300	20	140.00%

The first thing to look at is the concentration progress of the reactants. In the figures below, the concentration of the reactants and products can be seen. The values are presented mostly as averages of duplicates or triplicates:

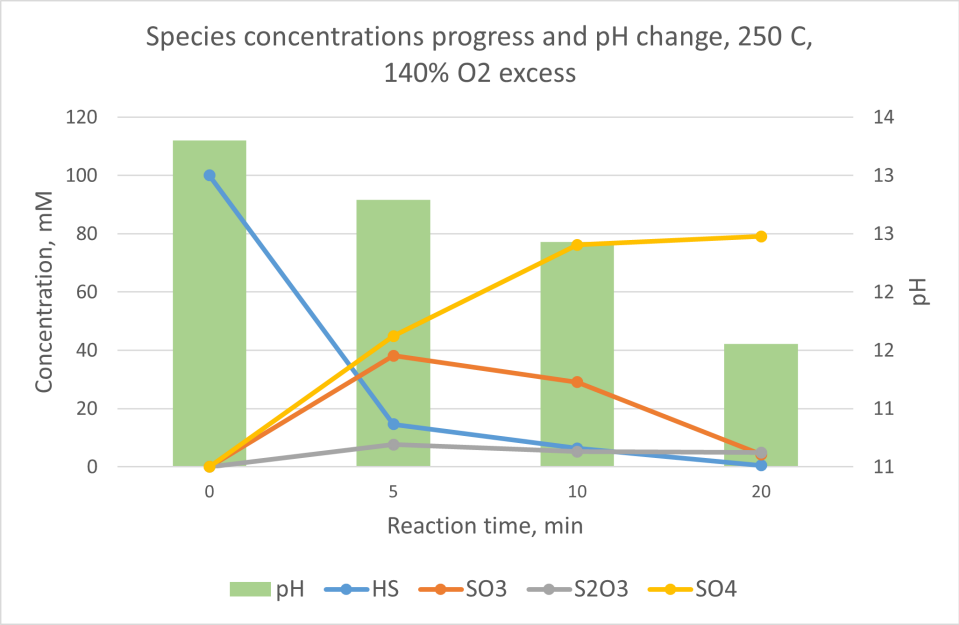

Figure 7.5: Species concentrations and pH at 250°C, P=90 bar

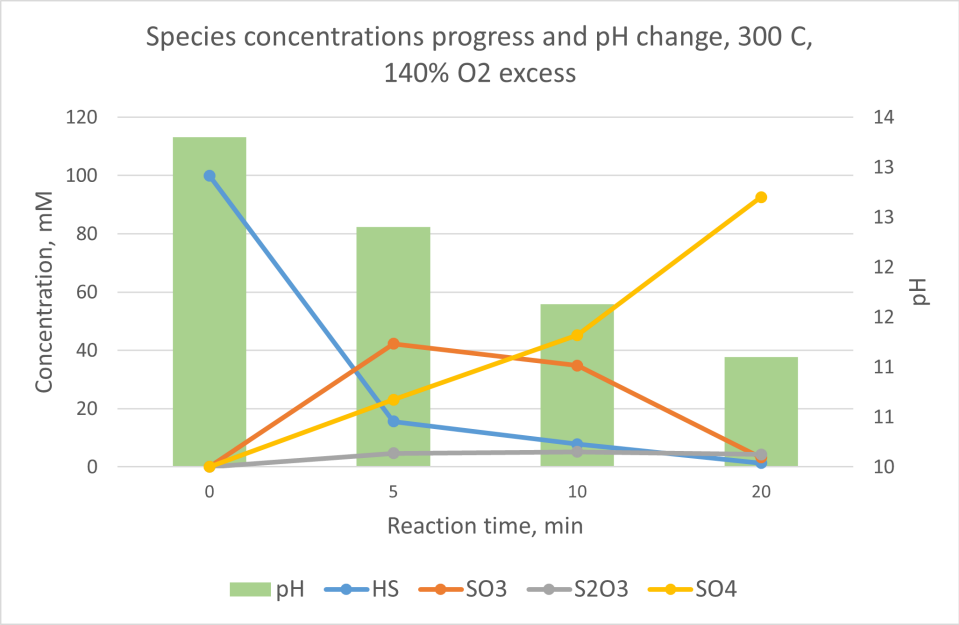

Figure 7.6: Species concentrations and pH at 300°C, P=150 bar

The pressures in those case were 90 and 150 bar. At 90 bar and 250°C the water density is 804 kg/m^3. At 150 bar and 300 °C the water density corresponds to 725 kg/m^3.

The first thing to notice is the pH. A sharper drop is experienced than for the first stage experiments. This is due to more bisulfide HS^- being converted.

As expected, the concentration of bisulfide decreases with reaction time. At 300°C there is almost no difference between the 2 levels of oxygen excess. At 250°C a faster consumption of the bisulfide is noticed at 200% excess. In both figures 7.5 and 7.6 it can be noticed that the biggest fraction of the bisulfide is consumed in the first 5 minutes.

Sulfite experiences a fast spike at 250°C in the first 5 minutes. A similar situation can be observed at 300°C. Further, the sulfite experiences a decrease. For both temperatures, the SO_3^{2-} decline is almost identical. This confirms again that sulfite is an intermediate compound.

Thiosulfate is also an intermediate products. Therefore, its concentration experiences an increase during the early stages, with a decrease later. At 250 °C, a spike is observed in 5 minutes. At 10 minutes, the concentration decreases for both temperatures. At 20 minutes, almost no thiosulfate is left.

Lastly, the sulfate concentration looks different than the previous ones. At 250°C, the concentration of sulfate increases faster with time. At 5 minutes, around 70% of thr final sulfate is formed. This is expected since the oxidation reaction progresses at higher temperatures. At 300 °C, the increase is not so sharp as for 250 °C, while the final amounts are similar.

Next, the experiments with higher oxygen levels are presented:

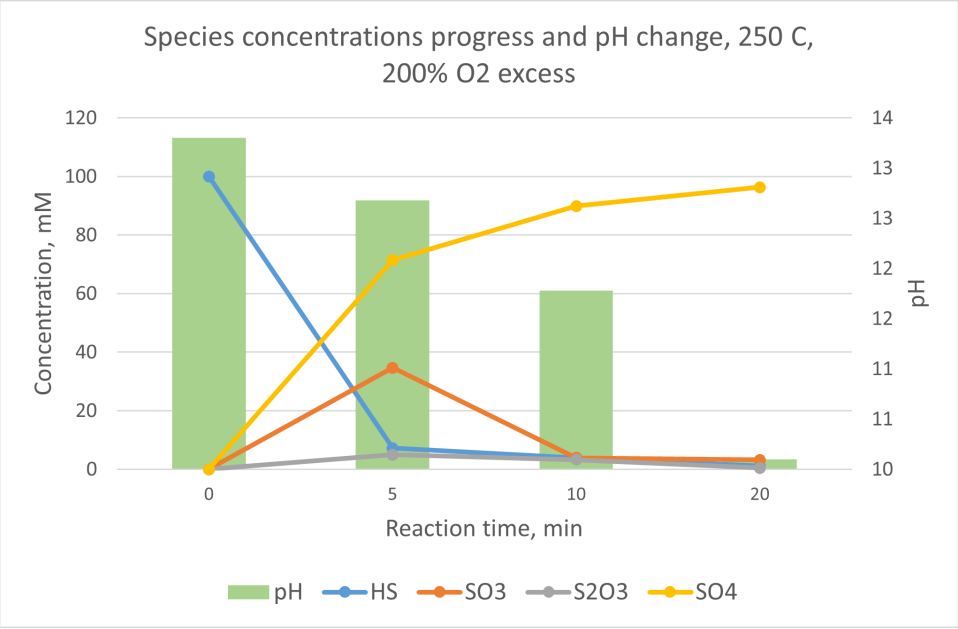

Figure 7.7: Species concentrations and pH at 250°C, P=130 bar

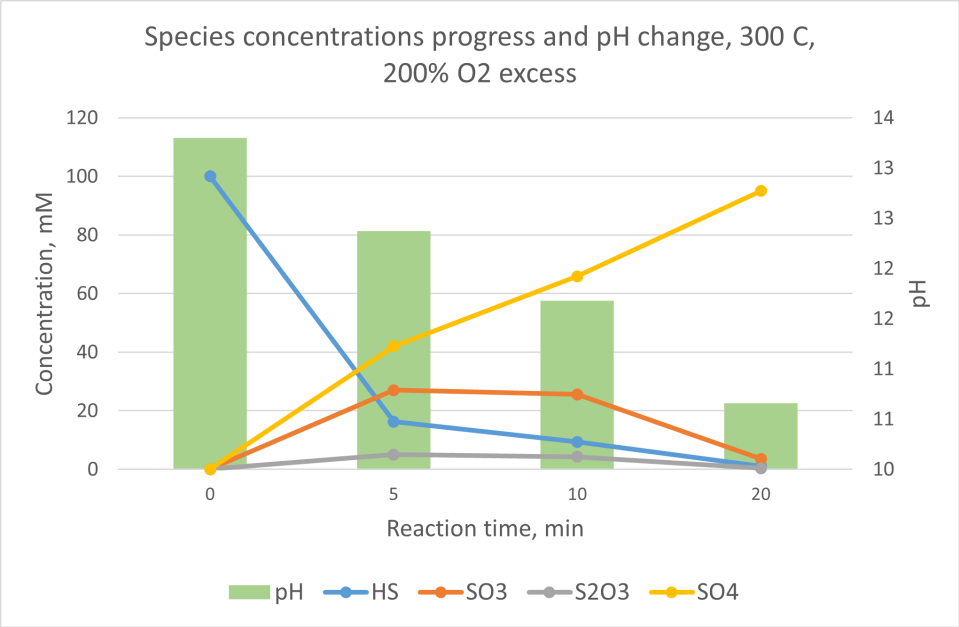

Figure 7.8: Species concentrations and pH at 300°C, P=190 bar

The pressures in those case were 130 and 190 bar. At 130 bar and 250°C the water density is 808 kg/m^3. At 190 bar and 300 °C the water density corresponds to 734 kg/m^3.

The pH trend for a higher oxygen level is similar, with a sharp decrease noticed towards 20 minutes reaction time.

The bisulfide concentration is decreasing very fast, with more than 90% being consumed in the first 5 minutes. At 300 °C a similar trend is observed.

The sulfite concentrations experience a sharp increase in the first 5 minutes for both temperatures. After that, their concentrations drops, peaking at 5 minutes reaction time.

Thiosulfate is not generated in large amount in both cases. It seems to be a very short-term intermediate products, with its concentration reaching 0 towards the end.

Finally, sulfate experience a sharper increase at 200% oxygen. Especially at 250°C, large amounts of SO_4^{2-} can be observed already at 5 minutes. For both temperatures, the final sulfate concentration almost equals the initial bisulfide concentration. This means that the oxidation is complete.

It is to be mentioned that the 300°C results look slightly off. It was expected that the oxidation reaction would proceed faster. An explanation is that at 300°C, the water has lower density, by around 100 kg/m^3. At higher densities, more oxygen is dissolved in the water. On the other hand, lower density ensures less oxygen in the liquid phase.

In addition, the selectivities are examined.

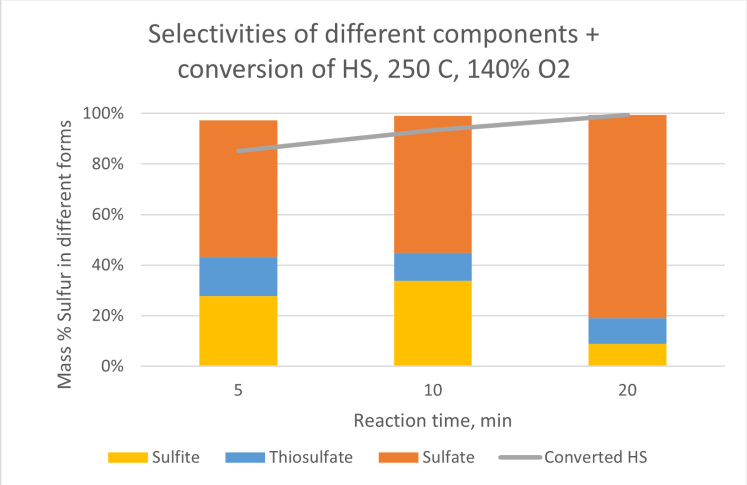

Figure 7.9: Selectivity and Sulfide conversion at 250°C and 140% oxygen excess

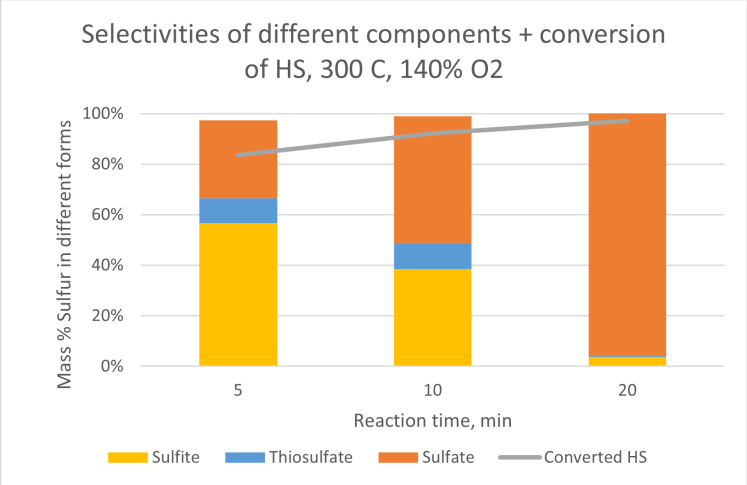

Figure 7.10: Selectivity and Sulfide conversion at 300°C and 140% oxygen excess

The selectivities confirm the previous results with each species' concentrations. As expected, at 20 minutes reaction time, the sulfate account for almost all of the detected sulfur. The difference is more prominent at higher temperatures. At 300 °C the sulfate is formed faster and in bigger amount.

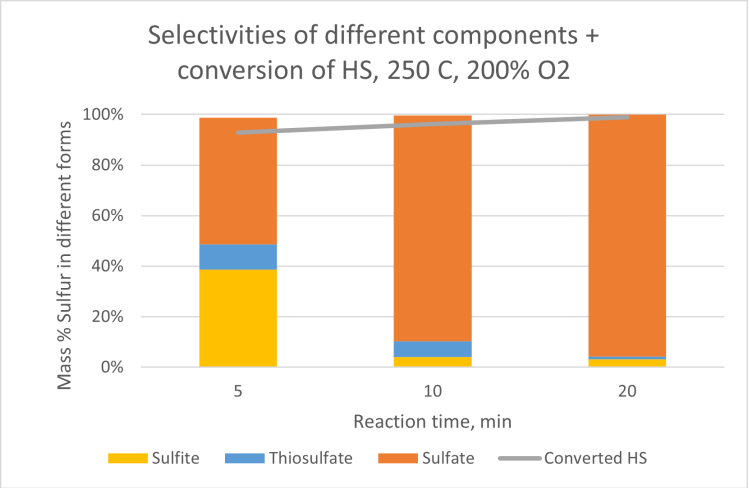

Figure 7.11: Selectivity and Sulfide conversion at 250°C and 200% oxygen excess

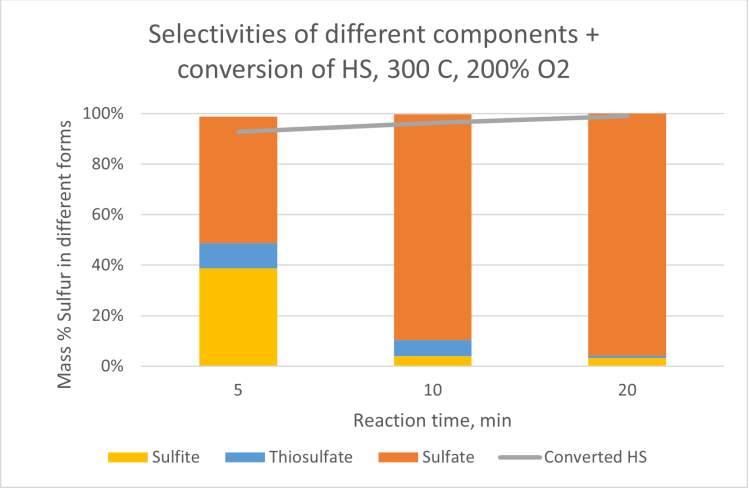

Figure 7.12: Selectivity and Sulfide conversion at 300°C and 200% oxygen excess

For 200% oxygen excess, the trend is similar to the 140%, where the sulfate only increases with time. However, at higher oxygen excess, the temperature does not play a big role, as the 250 and 300°C graphs look similar.

7.5 Temperature comparison

For the oxygen excess level of 140%, 4 temperature levels are available. Therefore, the comparison of the progress of the 4 analyzed components under different temperatures has also been looked at.

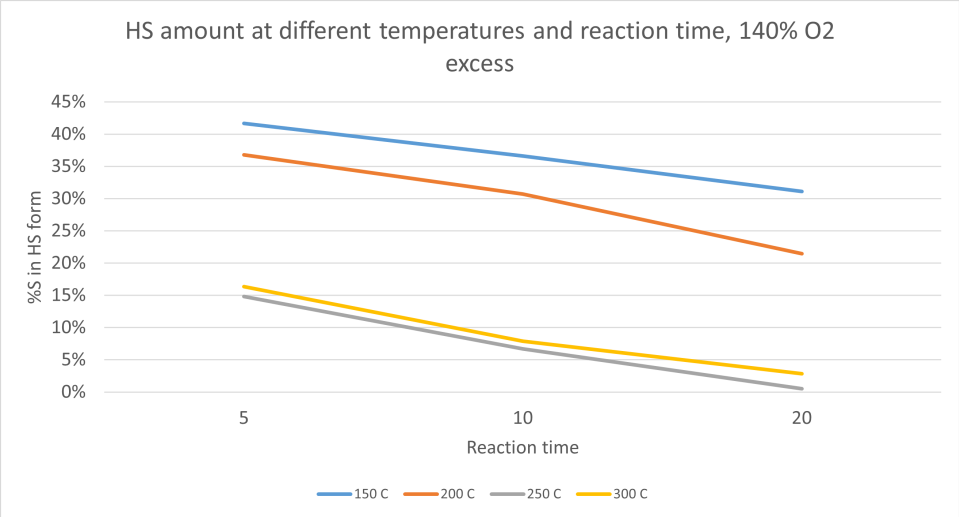

Figure 7.13: Bisulfide HS^- amount evolution at different temperatures

For all 4 temperature levels, the amount of HS^- drops with reaction time. For 250 and 300°C, the trends are very similar. The 250°C has even a slight edge over 300°C. This could be explained by the lower water density (804 vs 725kg/m^3) or errors in the 300°C experiments, as fewer repetitions were done at those conditions.

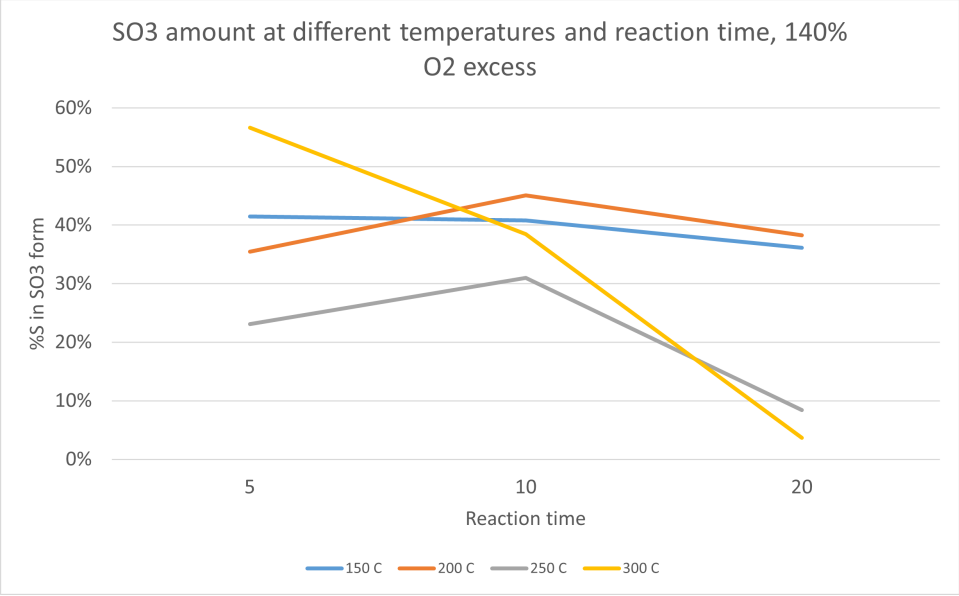

Figure 7.14: Sulfite SO_3^{2-} amount evolution at different temperatures

For sulfite (SO_3^{2-}), at 300°C the most is formed initially and it is also consumed the fastest in the end. The trend seems to be that at higher temperatures, more

sulfite is consumed in the end.

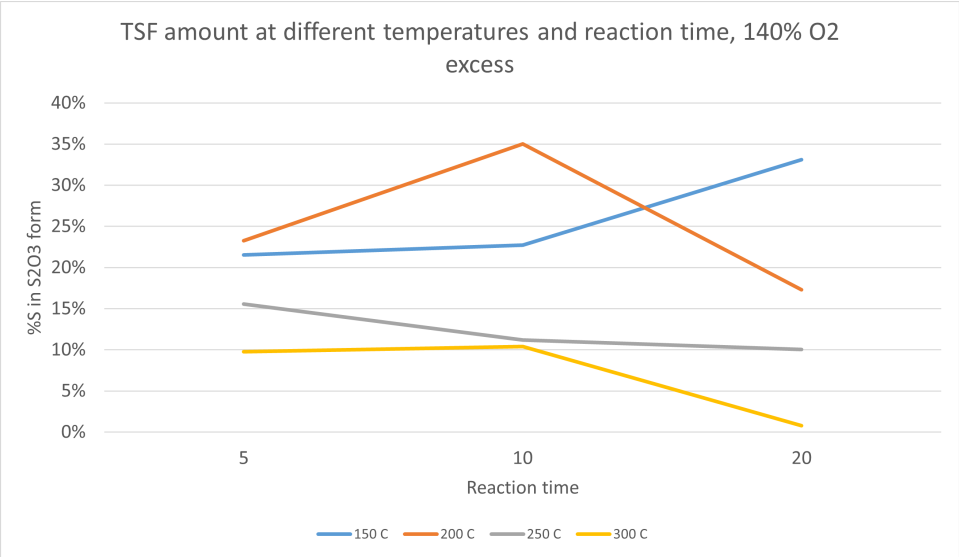

Figure 7.15: Thiosulfite $S_2O_3^{2-}$ amount evolution at different temperatures

Thiosulfate ($S_2O_3^{2-}$), just like sulfite, is an intermediate product. By the end it is expected to be consumed entirely and this is achieved at 300°C. At 150°C, as mentioned before, the thiosulfate does not reach a downward trend at 20 minutes. At the other times, it is generated at first, after which it is consumed.

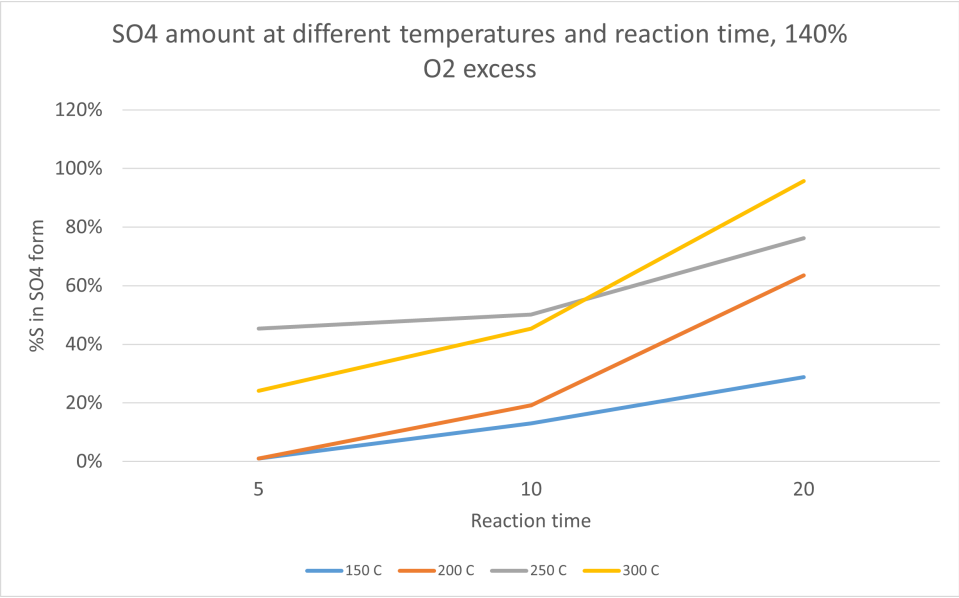

Figure 7.16: Sulfite SO_4^{2-} amount evolution at different temperatures

Sulfate (SO_4^{2-}) is the final oxidation product of the reaction. Towards the end, its amount should be similar to that of the initial bisulfide. This is achieved at 300°C. The sulfate amount in the end increases with temperature, which is expected, as reactions generally proceed faster at higher temperature values.

At 200%, similar graphs were made. However, only 2 temperature levels were available here.

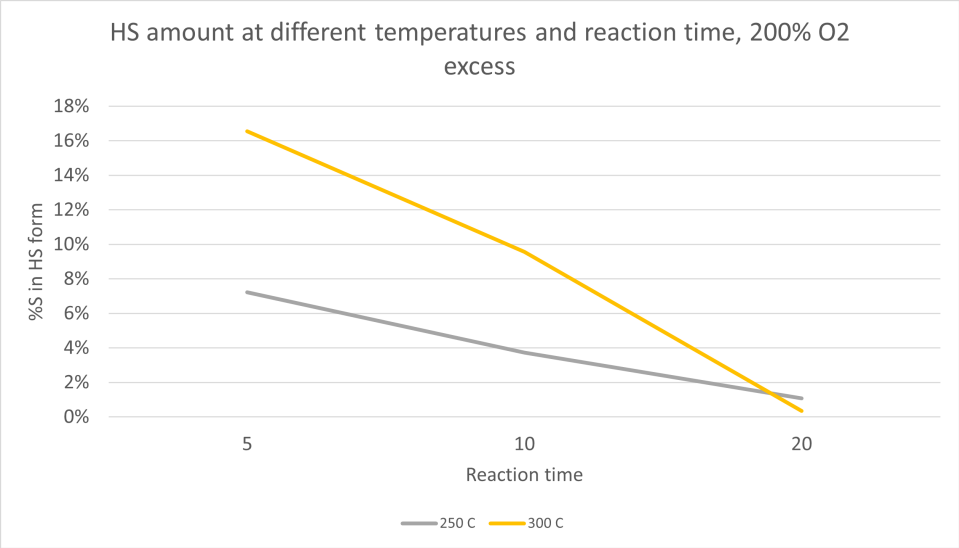

Figure 7.17: Bisulfide (HS^-) amount evolution at 250 and 300°C

At 250°C more (HS^-) is consumed at first. In the end, however, most of the bisulfide is consumed for both cases.

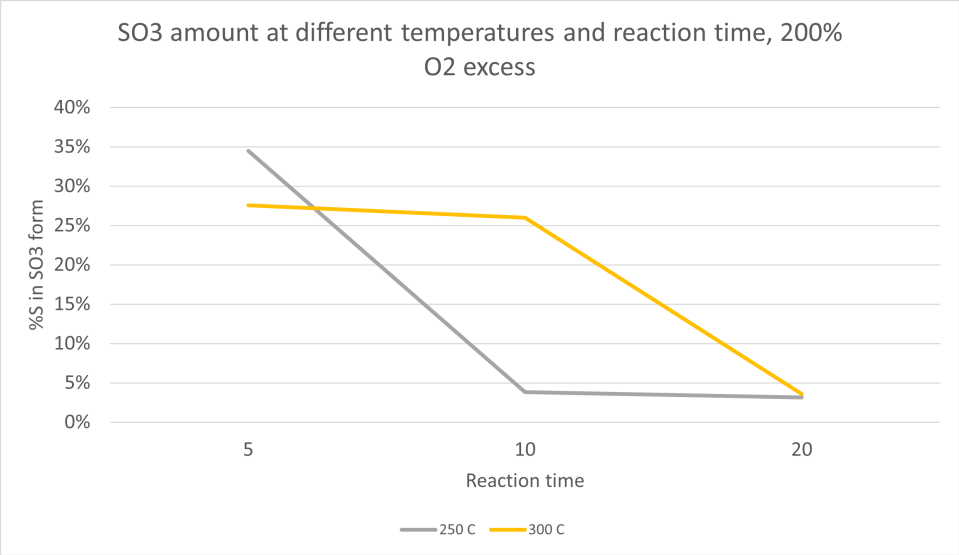

Figure 7.18: Sulfite (SO_3^{2-}) amount evolution at 250 and 300°C

Sulfite (SO_3^{2-}) is generated faster initially at 5 minutes at 250°C and then gets consumed almost entirely at 10 minutes. At 300°C a similar complete consumption is observed at 20 minutes. However, the process is slower. at 5 and 10 minutes.

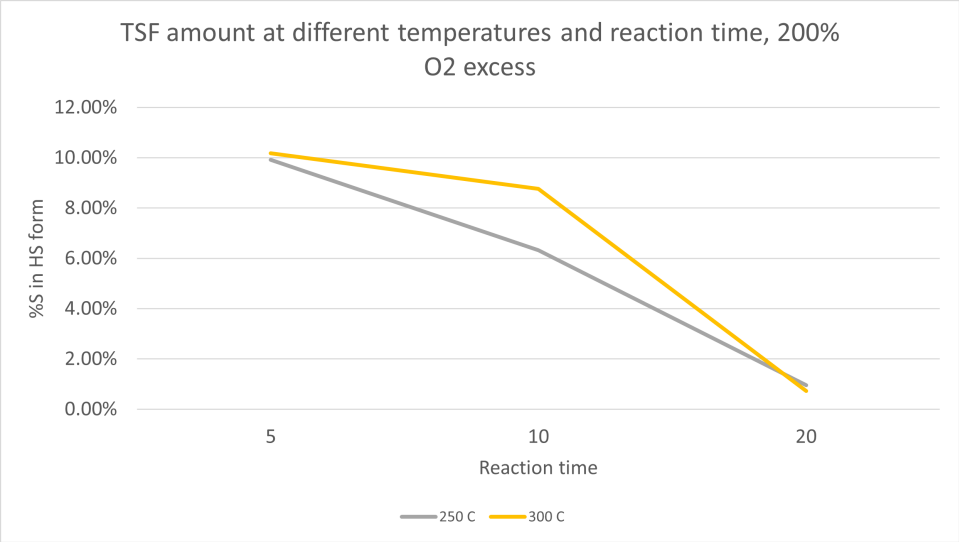

Figure 7.19: Thiosulfite ($S_2O_3^{2-}$) amount evolution at 250 and 300°C

The thiosulfite ($S_2O_3^{2-}$) trend looks similar for both temperatures. At 250°C, however, a faster consumption at 10 minutes is observed.

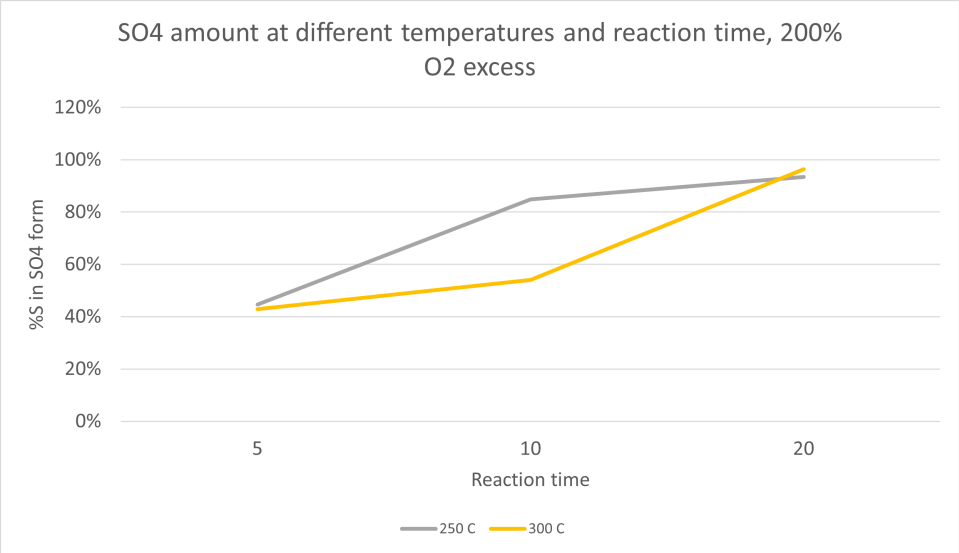

Figure 7.20: Sulfate (SO_4^{2-}) amount evolution at 250 and 300°C

Finally, sulfate (SO_4^{2-}), as the final oxidation product, is generated also faster at 250°C. Overall, the experiments performed at 250°C perform better than those at 300°C. As mentioned previously, the main reason for that could be the density difference, which interferes with the oxygen mass transfer.

7.6 Reaction Modeling Results

The integral method of analysis has been applied for the m values of 0, 1, 1.5, 2, 2.5 and 3. In the end, the first order provided the best R^2 and lowest intercept, for the 4 temperatures: 150, 200, 250 and 300°C. The used model was simplified under the assumption that the system is always saturated with oxygen, thus its concentration is to be ignored. In the figures below, the regression plot can be seen:

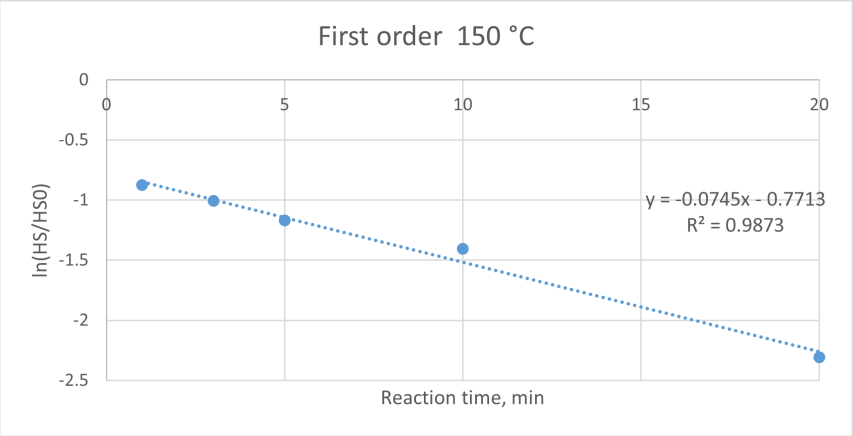

Figure 7.21: First order regression for 150°C

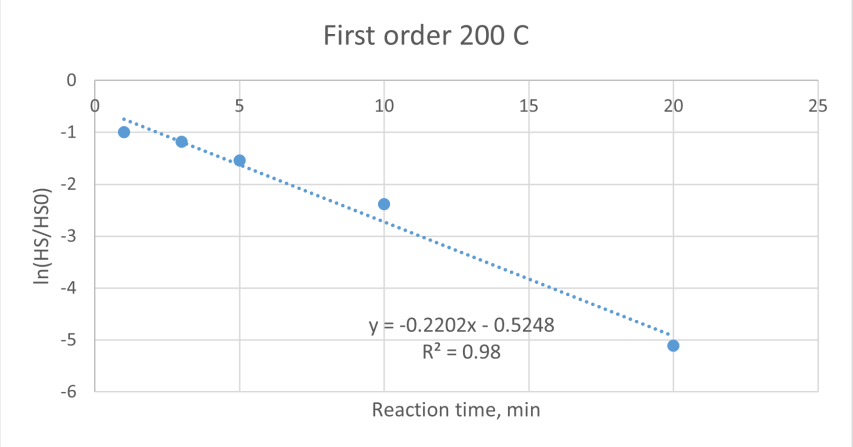

Figure 7.22: First order regression for 200°C

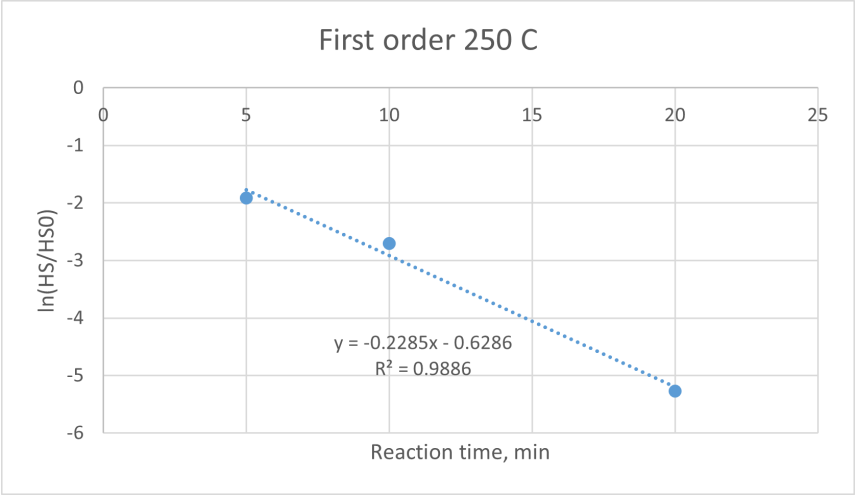

Figure 7.23: First order regression for 250°C

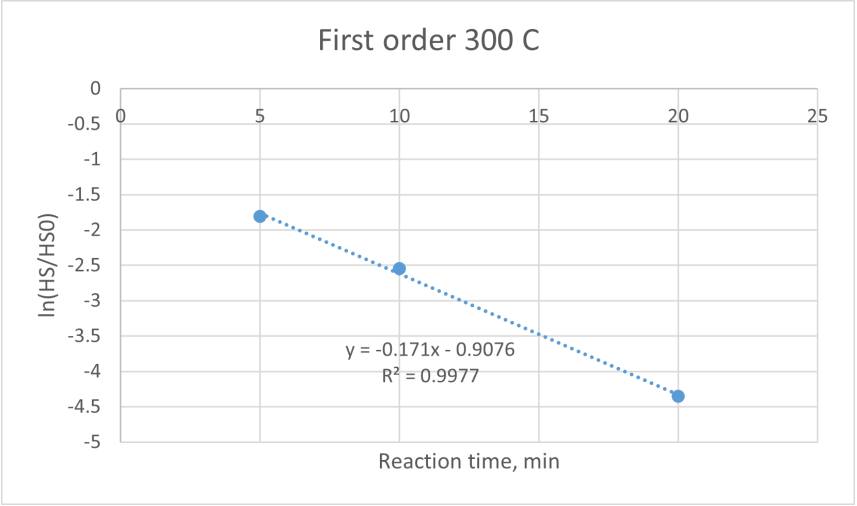

Figure 7.24: First order regression for 300°C

From the presented plots, the following k' values can be extracted:

Temperature (°C)	Oxygen excess (%)	k' (min^{-1})
150	140	0.0745
200	140	0.2202
250	140	0.2285
300	140	0.171

Table 7.3: k' values obtained for different temperature

From 150 to 200 $^{\circ}C$, the rate constant increases almost 3 times. This makes sense, because a temperature increase normally means an increase in reaction rate. For 250$^{\circ}C$ the rate increases but not by much. It is worth mentioning that the feed injected in the reactor was more for 250 and 300$^{\circ}C$. Therefore, the results between stage 1 and stage 2 are not entirely comparable. However, it is clearly noticed that from 250 to 300$^{\circ}C$, the rate constant has decreased. This does not correspond to the basic kinetic principles. As mentioned before, at 300$^{\circ}C$ the density of the water in the reactor was lower. This could impair the oxygen mass transfer, thereby deeming the oxygen saturation assumption untrue.

7.7 Discussion

The performed experiments had the goal to answer the research questions regarding which reaction conditions give better results and which reaction products are dominant in the effluents.

The obtained results from the experiments provide valuable inputs about the oxidation of the bisulfide ion. During the first stage experiments, it was confirmed that some of the components (Sulfite - SO_3^{2-} and thiosulfate - $S_2O_3^{2-}$) are temporary, as their concentrations curves have a convex structure, where they increase initially, after which they decrease. The final product of the oxidation is sulfate (SO_4^{2-}). Its concentration does not increase from the beginning, as the temporary components have to be formed first. Only after 5 minutes of oxidation, sulfate started to be seen. Hence, the second stage experiments were started from 5 minutes reaction time.

The most dominant effect was that of temperature, with results improving with increased temperature. Another parameters was the oxygen excess, which also generated the initial pressure. Higher oxygen levels mean higher pressure, which directly correlates to the solubility of oxygen in water. However, for temperatures too high, such as 300$^{\circ}C$, the temperature starts having an opposite effect. A likely explanation is the sharp density shift. From 250 to 300$^{\circ}C$, a change of almost 100 kg/m^3 can be seen. This most likely had an impact on the process. Lower density and higher temperature cause less oxygen to be dissolved in the liquid phase.

The reaction time also can be linked to different components present in the effluent. At lower reaction times, sulfites and thiosulfates dominate the system. With reaction progress however, sulfates become the dominant species. This can be traced back to the bisulfide oxidation reactions:

$$H_2S_{(aq)} \leftrightarrow HS^- + H^+ \tag{7.1}$$

$$HS^- + 1.5O_2 \rightarrow H^+ + SO_3^{2-} \tag{7.2}$$

$$SO_3^{2-} + 0.5O_2 \rightarrow SO_4^{2-} \tag{7.3}$$

$$SO_3^{2-} + HS^- + 0.5O_2 \rightarrow S_2O_3^{2-} + OH^- \tag{7.4}$$

$$S_2O_3^{2-} + 0.5O_2 \rightarrow SO_4^{2-} + S \tag{7.5}$$

The first reaction 7.1 determines the bisulfide present in the effluent. It also influences the pH. In this research, the bisulfide ion is already present in the solution. Hence, this reaction is not relevant. The oxidation of the bisulfide solution starts from reaction 7.2, as bisulfide ions are obtained from the sodium sulfide aqueous solution. Initially, the sulfites and thiosulfates are formed, then consumed. In the end, sulfate is the final product. At 20 minutes reaction time, for all temperatures, the most predominant component is sulfate. However, at $250^{\circ}C$ the best results are obtained in terms of % of initial bisulfide converted to sulfate.

The analysis performed in this research does not cover elemental sulfur. First, it is challenging to analyze. Second, it is believed that the last reaction 7.5 - the only one responsible for elemental sulfur generation had a very limited impact on the process. Due to low thiosulfate concentrations, the amount of elemental sulfur is likely to be small, causing errors below 5%. The value comes from the maximum thiosulfate concentration of 8 mM. Out of 100 mM of total bisulfide concentration, 8 mM account only for 8%. Further, half of those 8 mM went to sulfate formation, meaning less than 5 mM of potential elemental sulfur.

The modeling showed an increase in rate constant with temperature. The increase was however much larger from 150 to $200^{\circ}C$ than from 200 to $250^{\circ}C$. From 250 to $300^{\circ}C$ the rate decreased. The main potential reason for that is the density difference, which inteferes with the Oxygen mass transfer.

It is to be noted that for the $250^{\circ}C$ experiments, the reactor was charged with more bisulfide and oxygen overall. The excess was kept constant, but due to the vapor pressure increase, it was required to increase other parameters, such as bisulfide concentration and total amount of air inside, which resulted in higher pressure. Therefore, the results are not entirely comparable.

Chapter 8

Conclusion

The challenges in the oil and gas industry always create the demand for modern and innovative solutions. With the increasing environmental concerns, some of the processes in the industry are revised, due to their harmful effects. The H_2S treatment techniques used in offshore applications can have negative consequence on sea life, due to the residual chemicals being released in the sea. As a result, potential replacements have been researched.

This project focused on the hydrothermal oxidation of the bisulfide ion, as an alternative to its capture by scavengers and further release in the sea. The oxidation was performed on a small scale reactor, at different temperatures (150, 200, 250 and 300$^\circ C$) and reaction times (1, 3, 5, 10 and 20 minutes). The goal was to determine the most suitable conditions for the oxidation of bisulfide ions.

Initially, the results were poor, as lower temperatures were used. Later, with elevated temperatures and pressures, it was possible to determine which reaction conditions would be more suitable for reaching the experimental goal, which was to oxidize all the bisulfide and for all the sulfur to be in form of sulfate.

Throughout the research and analysis, the intermediate oxidation reaction products were quantified (sulfite -SO_3^{2-} and thiosulfate - $S_2O_3^{2-}$). Their dynamics are quite similar at all temperature. Initially, they form in abundance, but at higher oxidation times they convert into sulfate. The resulting effluent consisted primarily of sulfate ions, which are less harmful than the scavenger residues. Sulfate ions are often present in drinking water, making it perfectly safe. They are also present in the seawater, being one of the sources of sulfur in the hydrocarbon reservoirs.

The modeling provided rate constants for the different temperatures. The highest value was obtained at 250$^\circ C$, as the rate constant decreased at 300$^\circ C$. The results at 200$^\circ C$ are also quite good, with the reaction rate being just a little lower.

After more than 50 experiments and data analysis, was determined that at 250$^\circ C$ and 20 minutes of reaction time, the best results are obtained. Almost all of the sulfur ends up in sulfate form and no bisulfide is left. Therefore, in a potential

real-life bisulfide oxidation process, a bigger reactor operating at similar conditions could be used.

For energy efficiency, $200^{\circ}C$ could also be a suitable option. In terms of reaction time, 20 minutes seems to be the time when almost all the bisulfide disappears and is converted to sulfate. The oxygen level does not seems make a big difference, therefore 140% shall be used for energy efficiency.

References

[1] Jonathan Craig et al. "The history of the European oil and gas industry (1600s–2000s)". In: *Geological Society, London, Special Publications* 465.1 (2018), pp. 1–24. DOI: 10.1144/SP465.23. URL: https://www.lyellcollection.org/doi/abs/10.1144/SP465.23.

[2] Francis S Manning and Richard Thompson. "Oilfield processing". In: (1991).

[3] *Agency for Toxic Substances and Disease Registry*. URL: https://wwwn.cdc.gov/TSP/MMG/MMGDetails.aspx?mmgid=385&toxid=67#:$\sim$:text=Hydrogensulfideisavery,ofrespiratoryandcardiovascularfunctions..

[4] Rudolf H Hausler. "Contribution to the Understanding of H2S Corrosion". In: *NACE CORROSION*. NACE. 2004, NACE–04732.

[5] Obakore W Agbroko, Karishma Piler, and Tracy J Benson. "A Comprehensive Review of H2S Scavenger Technologies from Oil and Gas Streams". In: *ChemBioEng Reviews* 4.6 (2017), pp. 339–359. DOI: https://doi.org/10.1002/cben.201600026. URL: https://onlinelibrary.wiley.com/doi/abs/10.1002/cben.201600026.

[6] Mahsan Basafa and Kelly Hawboldt. "Reservoir souring: sulfur chemistry in offshore oil and gas reservoir fluids". In: *Journal of Petroleum Exploration and Production Technology* 9.2 (2019), pp. 1105–1118. ISSN: 21900566. DOI: 10.1007/s13202-018-0528-2. URL: http://dx.doi.org/10.1007/s13202-018-0528-2.

[7] Malcolm A Kelland. *Production Chemicals for the Oil and Gas Industry*. Second edi. Milton: CRC Press, 2014. ISBN: 9781439873793.

[8] Mahsan Basafa and Kelly Hawboldt. "Reservoir souring: sulfur chemistry in offshore oil and gas reservoir fluids". In: *Journal of Petroleum Exploration and Production Technology* 9.2 (2019), pp. 1105–1118.

[9] *Ullmann's Encyclopedia of Industrial Chemistry*, Volume A13, page 467. ISBN: 3-527-20113-0.

[10] John Spedding and Mary Vujcich. "Exchange of H2S between air and water". In: *Journal of Geophysical Research: Oceans* 87.C11 (1982), pp. 8853–8856.

[11] Antonio Zavarce. "Wet H2S damage mechanism: A comprehensive guide for industry professionals". In: *Inspenet* (). URL: https://inspenet.com/en/articulo/wet-h2s-damage-mechanism/.

[12] George Barger and Henry Hallett Dale. "Chemical structure and sympathomimetic action of amines". In: *The Journal of physiology* 41.1-2 (1910), p. 19.

[13] James G Speight. "Chapter 2 - Materials of Construction for Refinery Units". In: *Oil and Gas Corrosion Prevention*. Ed. by James G Speight. Boston: Gulf Professional Publishing, 2014, pp. 3–37. ISBN: 978-0-12-800346-6. DOI: https://doi.org/10.1016/B978-0-12-800346-6.00002-8. URL: https://www.sciencedirect.com/science/article/pii/B9780128003466000028.

[14] M. N. Shahrak, E. Ebrahimzadeh, and F. Shahraki. "Removal of Hydrogen Sulfide from Hydrocarbon Liquids Using a Caustic Solution". In: *Energy Sources, Part A: Recovery, Utilization and Environmental Effects* 37.8 (2015), pp. 791–798. ISSN: 15567230. DOI: 10.1080/15567036.2011.584121. URL: http://dx.doi.org/10.1080/15567036.2011.584121.

[15] R Álvarez-Cruz et al. "Insights in the development of a new method to treat H2S and CO2 from sour gas by alkali". In: *Fuel* 100 (2012), pp. 173–176. ISSN: 0016-2361. DOI: https://doi.org/10.1016/j.fuel.2012.05.009. URL: https://www.sciencedirect.com/science/article/pii/S0016236112003523.

[16] Joseph H Field et al. *Removing hydrogen sulfide by hot potassium carbonate absorption*. Vol. 5660. US Department of the Interior, Bureau of Mines, 1960.

[17] Dong-Cheon Seo, Ruifeng Guo, and Dong-Hoon Lee. "Performance of alkaline impregnated biochar derived from rice hull for hydrogen sulfide removal from gas". In: *Environmental Engineering Research* 26.6 (2021).

[18] Xiaoting Wang et al. "Elucidating the reaction mechanisms between triazine and hydrogen sulfide with ph variation using mass spectrometry". In: *Analytical chemistry* 90.18 (2018), pp. 11138–11145.

[19] *European Chemicals Agency*. URL: https://echa.europa.eu/da/substance-information/-/substanceinfo/100.208.078.

[20] Adrian Wright Kim Rasmussen and Henning Lund Mick Schofield. "INVESTIGATION OF A CORROSION FAILURE IN AN OFFSHORE GAS COMPRESSION SYSTEM: THE ROLE OF H2S SCAVENGER AND ORGANIC ACIDS". In: *Corrosion* 04059 (2004), p. 13.

[21] *European Chemicals Agency*. URL: https://echa.europa.eu/da/substance-information/-/substanceinfo/100.208.078.

[22] *European Chemicals Agency*. URL: https://echa.europa.eu/da/substance-information/-/substanceinfo/100.208.078.

[23] Marko Stipanicev et al. “Multifunctional H2S scavenger and corrosion inhibitor: addressing integrity challenges and production output of the mature field”. In: *SPE International Oilfield Corrosion Conference and Exhibition*. SPE. 2018, D011S001R001.

[24] Iveth Romero, Sergey Kucheryavskiy, and Marco Maschietti. “Experimental study of the aqueous phase reaction of hydrogen sulfide with MEA-triazine using in situ Raman spectroscopy”. In: *Industrial & Engineering Chemistry Research* 60.43 (2021), pp. 15549–15557.

[25] S T Kolaczkowski et al. “Wet air oxidation: a review of process technologies and aspects in reactor design”. In: *Chemical Engineering Journal* 73.2 (1999), pp. 143–160. ISSN: 1385-8947. DOI: https://doi.org/10.1016/S1385-8947(99)00022-4. URL: https://www.sciencedirect.com/science/article/pii/S1385894799000224.

[26] M M M’Arimi et al. “Recent trends in applications of advanced oxidation processes (AOPs) in bioenergy production: Review”. In: *Renewable and Sustainable Energy Reviews* 121 (2020), p. 109669. ISSN: 1364-0321. DOI: https://doi.org/10.1016/j.rser.2019.109669. URL: https://www.sciencedirect.com/science/article/pii/S1364032119308743.

[27] Jia-Zhong Zhang and Frank J Millero. “The products from the oxidation of H2S in seawater”. In: *Geochimica et Cosmochimica Acta* 57.8 (1993), pp. 1705–1718. ISSN: 0016-7037. DOI: https://doi.org/10.1016/0016-7037(93)90108-9. URL: https://www.sciencedirect.com/science/article/pii/0016703793901089.

[28] M Avrahami and RM Golding. “The oxidation of the sulphide ion at very low concentrations in aqueous solutions”. In: *Journal of the Chemical Society A: Inorganic, Physical, Theoretical* (1968), pp. 647–651.

[29] AT Kuhn, MS Chana, and GH Kelsall. “A review of the air oxidation of aqueous sulphide solutions”. In: *Journal of Chemical Technology and Biotechnology. Chemical Technology* 33.8 (1983), pp. 406–414.

[30] Norman Neill Greenwood and Alan Earnshaw. *Chemistry of the Elements*. Elsevier, 2012.

[31] Ilari Filpponen et al. “Spectral monitoring of the formation and degradation of polysulfide ions in alkaline conditions”. In: *Industrial & engineering chemistry research* 45.22 (2006), pp. 7388–7392.

[32] Joachim Weiss. *Handbook of Ion Chromatography, 3 Volume Set*. Vol. 1. John Wiley & Sons, 2016.

[33] NK Boardman. “Ion-exchange chromatography”. In: *Modern Methods of Plant Analysis/Moderne Methoden der Pflanzenanalyse*. Springer, 1962, pp. 159–204.

[34] *What is Raman Spectroscopy?* URL: https://www.edinst.com/blog/what-is-raman-spectroscopy/.

[35] Andrzej Kudelski. "Analytical applications of Raman spectroscopy". In: *Talanta* 76.1 (2008), pp. 1–8. ISSN: 0039-9140. DOI: https://doi.org/10.1016/j.talanta.2008.02.042. URL: https://www.sciencedirect.com/science/article/pii/S0039914008001641.

[36] Michael Thompson. *Handbook of inductively coupled plasma spectrometry*. Springer Science & Business Media, 2012.

[37] Nikolaos Montesantos et al. "Proof of concept of hydrothermal oxidation for treatment of triazine-based spent and unspent H2S scavengers from offshore oil and gas production". In: *Chemical Engineering Journal* 427 (2022), p. 131020.

[38] National Institute of Standards and Technology. *Security Requirements for Cryptographic Modules*. Tech. rep. Federal Information Processing Standards Publications (FIPS) 140-2, Change Notice 2 December 03, 2002. Washington, D.C.: U.S. Department of Commerce, 2001. DOI: 10.6028/nist.fips.140-2.

Appendix A

Appendix A

View attachments for a detailed table of the results.